2015

Changes to parvalbumin neurons in the prefrontal cortex and reticular thalamus in the neonatal ventral hippocampal lesion model of schizophrenia

Hannaford Edwards, Integrated Program in Neuroscience,
McGill University
July, 2015

A thesis submitted to McGill University in partial fulfillment of the requirements of the degree of Master's of Science

Table of Contents

Proposal abstract

Schizophrenia is a debilitating disorder with a life-time prevalence of approximately 0.5-1% worldwide. Diagnosis usually occurs in early adulthood and is based on the presentation of classical symptoms. Schizophrenia has a complex etiology involving multiple genes, neurotransmitter systems, and a number of different brain areas. Inhibitory GABA neurons, and the parvalbumin-positive (PV+) subset in particular, are disrupted in a number of crucial brain areas. Both human and animal studies of schizophrenia have found reductions in PV+ neuron markers, along with alterations in GABA synthesizing enzyme (GAD67) and receptor profiles, in the prefrontal cortex (PFC), an area involved in higher cognitive function and executive planning. The reticular nucleus (Rt), a PV-neuron rich relay nucleus of the thalamus, connects with the PFC and other brain areas to provide important modulatory control for thalamo-cortical and cortico-thalamic circuits. The role of the Rt in attention, consciousness, and sleep also suggests it may be disrupted in schizophrenia. Alterations to PV+ and GABA+ neuron numbers in the PFC and Rt have yet to be investigated in a robust animal model of schizophrenia, particularly in adolescence before the onset of schizophrenia-relevant behaviour. Accordingly, the aim of my thesis work was to quantitatively analyze PV- and GAD67-expressing neurons in the PFC and Rt of adolescent (PD20) and adult (PD60) animals in a rat neonatal hippocampal lesion model of schizophrenia. It was hypothesized that PV and GAD67 staining would be reduced in both the PFC and Rt in lesion animals, with a greater loss of expression in adulthood, after behavioural changes, relative to adolescence. A reduction in GAD67+ neurons in the prelimbic area of the PFC in adolescence was found ($p<0.015$), but otherwise no change was uncovered between sham and lesion animals in the PFC. Though PV+ numbers in the PFC stayed the same, these neurons may not express GAD67, or can lose their functionality in other ways. In the Rt, a dramatic loss of over 50% of PV+ neurons was seen at both age points ($p<0.00013$), with particular loss in the ventro-lateral region of this nucleus. This is the first time molecular changes to the Rt have been observed in an animal model of schizophrenia. Going forward, the PFC-thalamus-hippocampus circuit is a promising area for future schizophrenia research.

Résumé

La schizophrénie est une maladie débilitante avec une prévalence de la durée de vie d'environ 0,5-1% dans le monde. Le diagnostic se produit généralement chez l'adulte jeune et est basé sur la présentation de symptômes classiques. La schizophrénie a une étiologie complexe impliquant de multiples gènes, les systèmes de neurotransmetteurs, et un certain nombre de différentes zones du cerveau. Neurones GABA inhibiteur, et la (PV +) sous-ensemble de la parvalbumine-positifs, en particulier, sont perturbés dans un certain nombre de régions du cerveau cruciales. Les deux études humaines et animales de la schizophrénie ont constaté des réductions de PV + neurones marqueurs, avec des altérations dans enzyme de synthèse du GABA (GAD67) et les profils des récepteurs, dans le cortex préfrontal (PFC), une région impliquée dans la fonction cognitive plus élevé et de la planification de la direction. Le noyau réticulaire (Rt), un PV-neurone riche relais noyau du thalamus, se connecte avec le PFC et d'autres zones du cerveau pour fournir un contrôle de modulation important pour les circuits thalamo-corticales et cortico-thalamiques. Le rôle de la Rt dans l'attention, la conscience et le sommeil suggère aussi il peut être perturbé dans la schizophrénie. Modifications de PV + et + neurones GABA numéros dans le PFC et Rt doivent encore être étudiés dans un modèle animal robuste de la schizophrénie, en particulier à l'adolescence avant l'apparition du comportement de la schizophrénie pertinentes. En conséquence, le but de mon travail de thèse était d'analyser quantitativement et PV- neurones exprimant GAD67 dans le PFC et Rt de l'adolescent (PD20) et adultes (PD60) animaux dans un modèle rat nouveau-né de la lésion de l'hippocampe de la schizophrénie. Il a été émis l'hypothèse que les PV et GAD67 coloration serait réduit à la fois dans le PFC et Rt chez les animaux de lésions, avec une plus grande perte de l'expression à l'âge adulte, après des changements de comportement, par rapport à l'adolescence. Une réduction de GAD67 + neurones dans la région prélimbique du PFC à l'adolescence a été trouvée ($p < 0,015$), mais sinon aucun changement n'a été découvert entre les faux et lésions animaux dans le PFC. Bien que nombre PV + dans le PFC sont restés les mêmes, ces neurones ne peuvent pas exprimer GAD67, ou peuvent perdre leur fonctionnalité dans d'autres façons. Dans le Rt, une perte dramatique de plus de 50% des neurones PV + a été vu à deux points de l'âge ($p < 0,00013$), avec notamment la perte dans la région ventro-latérale de ce noyau. Ceci est la première fois que des changements moléculaires à la Rt ont été observés dans un modèle animal de la schizophrénie. À l'avenir, le circuit PFC-

thalamus-hippocampe est un domaine prometteur pour les futures recherches sur la schizophrénie.

Acknowledgements

A huge thank-you to Sanjeev Bhardwaj and Poonam Sharma for training me in the lab techniques used in this thesis and helping me through the slippery parts.

Thank you to my committee members Dr. Sylvain Williams and Dr. Tak Pan Wong for their unique insight and challenging questions during the development of this project.

I am tremendously grateful to my supervisor Dr. Lalit Srivastava for providing me with support, ideas, experience, and encouragement to complete this research. I would also like to thank him and the Canadian Institutes of Health Research for the financial support of this project.

Finally I would like to thank all the wonderful friends I've made here in Montreal who have kept me stable, and Kosta Gligorijevic for his patience and love over the past three years.

Introduction

Schizophrenia is one of the most widespread psychiatric disorders, with 0.5-1% of the world population affected (Gonzales-Burgos et al., 2011). With over 100 years of research into this disorder, there is still no clear cause or fully successful treatment method. Although symptoms generally appear in late adolescence to early adulthood and persist throughout life, it is believed that schizophrenia is in fact a developmental disorder (Curley and Lewis, 2012). It is a spectrum disorder, like autism, with various severities and manifestations of symptoms, along with many genes and other pathologies associated with the development of the disorder (Kendler, 2014). Notable genes associated with the disorder are those involved in brain development and maturation, such as DISC1, neuregulin and dysbindin, traditionally discovered through studies of families with high rates of bipolar, schizo-affective and schizophrenia disorders (Kendler, 2014). Early pre- and post-natal insults can also increase the risk for schizophrenia, including maternal infection, maternal famine, early life infection, and perinatal stress (Tseng et al., 2009). Being a spectrum disorder, it is the interaction between various environmental insults and low-level risk genes that manifests in symptoms (Kendler, 2014). Diagnosis is based on the presentation of a combination of classical symptoms, since no singular gene, environmental insult or brain scan is pathognomic of the disorder. While positive symptoms like paranoia and hallucinations are traditionally associated with the disorder, negative symptoms such as social withdrawal and anhedonia along with cognitive deficits are also present (Fallon et al., 2003). Although more difficult to test for and to treat, cognitive symptoms – including working memory deficits, reduced executive function and altered attention – appear earliest in illness progression and are a robust predictor of severity (Curley and Lewis, 2012).

Prefrontal Cortex

It is theorized that the late onset of symptoms in schizophrenia, despite being a developmental disorder, is due to the fact that the disrupted pathways and connections are some of the last to reach maturity (Curley and Lewis, 2012). The prefrontal cortex (PFC) in particular is one of the last cortical areas to mature, with complex circuit refinement and synaptic pruning ending in late adolescence – around the same time as typical schizophrenia symptom onset (Gogtay et al., 2004). The PFC is involved in many sophisticated tasks associated with symptoms of schizophrenia, particularly emotional processing and traits involved in cognitive symptoms (Gonzales-Burgos et al., 2011). The protracted development of the PFC throughout adolescence increases the vulnerability to postnatal developmental upset, which can manifest in a variety of ways. In adults with schizophrenia, a decrease in global connectivity at resting state is seen in the PFC, with the level of disconnect increasing with increased severity of negative and depressive symptoms (Hinkley et al., 2011). Patients also show decreased connectivity within the PFC while performing a working memory task (Grillon et al., 2013). In a 2- or 4-choice based reaction time test to analyze processing speed, which also takes into account attention and working memory, schizophrenic patients had a much slower processing speed and abnormal hyperactivity within the PFC during the task compared to matched controls (Woodward et al., 2013). While both imaging and post-mortem studies have shown a decrease in PFC volume (Ohtani et al., 2014; Selemon et al., 2002), the changes are subtle and suggest that schizophrenic symptoms are more likely due to connectivity or neurotransmitter system dysfunction than gross cortical loss.

Prefrontal cortex divisions

The medial PFC of rats is believed to be homologous to the dorsolateral PFC of primates, which appears to be responsible for most the above behaviours of schizophrenia (Heidbreder and Groenewegen, 2003). In rats, the mPFC separated into three subregions: the cingulate, prelimbic and infralimbic cortices. Each region forms connections with different subcortical areas, and disruption of particular connections or subcortical areas may result in differences in behavioural outcome or symptoms (Godsil et al., 2013). The cingulate connects to orbital regions and is thus believed to be involved predominantly in eye movement control (Heidbreder and Groenewegen, 2003), although rats with cingulate cortex lesions also show deficits in temporo-spatial memory and attentional selectivity (Dalley et al., 2004). The prelimbic area projects to the nucleus accumbens, nucleus reuniens, olfactory areas and VTA, and receives input from ventral CA1 and subiculum of the hippocampal formation. This broadly means that it is involved in cognitive functions and working memory, and specifically affects executive function (Dalley et al., 2004). Finally the infralimbic area projects to amygdala, midline thalamus, brainstem and hypothalamus, and receives input from CA1 and subiculum. It is involved in viscero-motor functions, as well anxiety and stress with the prelimbic area (Vertes, 2004). Changes to one of these regions selectively would result in distinct behavioural and downstream connectivity outcomes.

GABA neurons

One neurotransmitter system that appears affected in schizophrenia is the inhibitory γ-aminobutyric acid (GABA) system, which reaches maturity by end of adolescence in the cortex and plays an important role in signalling throughout development (Gandal et al., 2012). GABA

interneurons make up 20-30% of cortical neurons and provide essential inhibitory control in the cortex, including the modulation of PFC firing through circuits with the glutamate and dopamine systems (Nakazawa et al., 2012). GABA is produced in interneurons by two forms of glutamic acid decarboxylase (GAD): constitutive GAD67, ubiquitously expressed in the cell throughout development into adulthood, and inducible GAD65, expressed mostly in synaptic boutons later in development (Pinal and Tobin, 1998). The balance of excitation and inhibition is necessary for healthy brain function, and disruption of this balance is implicated in many mental disorders.

A number of post-mortem studies have reported deficits in the GABA system in schizophrenia, particularly in the PFC. While one study found GABA(A) α-1 receptor subunit mRNA levels to be elevated in schizophrenia post-mortem (Ohnuma et al., 1999), a more recent analysis of these mRNA levels found an overall decrease in the PFC, cingulate, motor and visual cortices (Hashimoto et al., 2008). The vesicular GABA transporter (VGAT), which fills presynaptic vesicles with GABA, shows reduced mRNA levels overall in patients, with a greater reduction in the PFC (Curley et al., 2013; Ohnuma et al., 1999). Decreased binding to GABA receptors is also observed in the frontal and temporal cortices in patients (Nikolaus et al., 2014). A decrease in GAD67 mRNA and protein has been seen in the amygdala, nucleus accumbens (NAcc) and thalamus of patients with schizophrenia, along with many cortical areas (Blum and Mann, 2002; Perry et al., 1979; Curley et al., 2013). These findings all support the potential of GABA dysfunction in schizophrenia, with particular disruption in the PFC.

GABA neurons are divided into three generally non-overlapping subtypes based on the expression of calcium-binding proteins: parvalbumin-positive (PV+), somatostatin-positive (SST+) and calretinin(CR+)/cholesystokinin-positive (CCK+) neurons (DeFelipe et al., 2013). Each subtype has different functionality, while neurons with different morphological

characteristics, including basket, chandelier and arcade cells, are found within each subtype (DeFelipe et al., 2013). About 50% of cortical GABA neurons are PV-positive, and these appear to be particularly affected in schizophrenia.

Parvalbumin neurons

The PV interneuron subtype contains two distinct cell morphologies: basket cells and chandelier cells. Both cell types are characterized by their high-frequency, non-adaptive firing, which distinguishes them as fast-spiking (FS) neurons (Povysheva et al., 2013). Basket cells release GABA onto the soma and proximal dendrites of glutamatergic pyramidal neurons, which produces a fast post-synaptic response, while chandelier cells synapse at the axon hillock of excitatory pyramidal cells and modulate cell response (Curley and Lewis, 2012). Although GAD67 mRNA levels in the PFC of schizophrenia patients are not decreased overall when compared to matched control, a 50% reduction in GAD67 mRNA is particular to PV+ axon terminals (Hashimoto et al., 2003). PV mRNA itself is also reduced in the PFC of patients with schizophrenia (Volk et al., 2012). GABA transporter-1 (GAT-1), a plasma membrane transporter which is responsible for the reuptake of GABA into presynaptic terminals, has significantly reduced mRNA levels in PV+ neurons relative to overall GAT-1 levels in the PFC (Volk et al., 2001; Bitanihirwe and Woo, 2014). PV+ cells appear to be responsible for synchronizing cortical γ rhythms (30-50 Hz), which are disrupted in schizophrenia (Sun et al., 2011). γ oscillations in the cortex play an important role in a number of higher cognitive tasks including working memory, attention and selection, and refining executive function, all which are affected in schizophrenia (Bartos et al., 2007). A reduction in excitatory glutamatergic signaling onto PV+ neurons in the PFC has been suggested through post-mortem studies which, along with elevated levels of hyperpolarizing μ opioid receptor mRNA in PV+ neurons, could contribute to an

imbalance of excitation and inhibition in schizophrenia and potentially disrupted γ rhythms (Bitanihirwe et al., 2009; Volk et al., 2012). These numerous findings support GABA, and PV in particular, hypofunction in the PFC in schizophrenia. Investigating when PV or GABA expression loss occurs in the PFC in a robust animal model of schizophrenia would help to provide insight into PV+ neuron changes in schizophrenia, as well as support the validity of the animal model.

Reticular Thalamus

The interconnectedness of the PFC with many cortical and subcortical areas implicates it in the integration of multiple sensory inputs and in cognitive control of appropriate responses (Gonzales-Burgos et al., 2011). Disrupted connections from the hippocampus and other subcortical brain areas to the PFC appear to play a role in symptom development, likely arising from disrupted formation of normal brain circuitry (Fallon et al., 2003). One subcortical area, the reticular thalamic nucleus (Rt, also abbreviated as TRN in the literature), receives many connections from with the prefrontal cortex along with a large number of other cortical and sub-cortical regions (Zikopoulos and Barbas, 2007). This thin, shell-shaped nucleus is solely an output nucleus, with no interneurons within the Rt. However, axon collaterals and chemical synapses connect neurons in the Rt to each other, which allows the Rt to produce both single-spike and burst-spike firing (Zikopoulos and Barbas, 2007). The Rt is known to receive connections from PFC, hippocampal formation, thalamus, and brainstem, and projects to thalamic nuclei and cortex (Pinault, 2004). It is ideally located between the white matter and the internal thalamic nuclei to play an important role modulating information transfer in both cortico-thalamic and thalamo-cortical circuits (Min, 2010).

Interestingly, the Rt is composed entirely of inhibitory GABA-ergic neurons, the majority of which are PV+ (~70%; Arai et al., 1994). Although some SST+ and CB+ neurons are also seen, they are sparse and not functionally distinct (Arai et al., 1994). PV staining in the Rt is present on PD0 in rats, centrally located but spreading caudally then rostrally as the animal matures (Majak et al., 1998). This GABA-ergic nucleus provides strong inhibitory power to the dorsal nuclei of the thalamus. Inputs to the Rt from the cortex and outputs from the Rt to the thalamus are generally arranged topographically, although there some overlap or 'blurring' in the topography, particularly in circuits with higher-order association cortices (Zikopoulos and Barbas, 2007).

The Rt acts as an interface or collateral between the cortex and the thalamus for practically all functional modalities (Pinault, 2004). Given this integrative role, there are theories that the Rt is involved in awareness of consciousness (Min, 2010). It is known that the Rt is involved in attention and attentional shift, a common symptom in schizophrenia (Ferrarelli and Tononi, 2011). Burst-spike firing in the Rt is responsible for sleep spindles, which characterize non-REM sleep and are dysfunctional in schizophrenia patients (Ferrarelli et al., 2010). The spiking properties of the Rt are also involved in producing thalamic gamma rhythms, which influence cortical gamma rhythms and appear during hallucinations (Behrendt, 2006). The role of the Rt in attention, sleep states and potentially consciousness also implicate it as a vulnerable centre for hallucinations in schizophrenia (Behrendt, 2006).

A recent study lesioning the dorsal-caudal region of the Rt found reduced pyramidal cell spines in the PFC, NAcc, and hippocampus, along with reduced dendritic length in the PFC and NAcc (Torres-Garcia et al., 2012). This group also found reduced exploratory behaviours in animals with an Rt lesion, while previous lesion studies have also seen behavioural neglect

(Torres-Garcia et al., 2012; Behrendt, 2006). The glutamate receptor antagonist phencyclidine (PCP) reduces the discharge rate of Rt neurons to about 37% of baseline (Troyano-Roriguez et al., 2014), while chronic PCP administration is associated with decreased PV mRNA in the Rt and impaired attentional shifting in rats (Egerton et al., 2005). These findings all suggest a change to the Rt in schizophrenia, but the developmental timing and extent of any potential alterations are still unknown.

Neonatal ventral hippocampal lesion

Our laboratory has developed and used a well-validated animal model of schizophrenia which mimics schizophrenic-like behaviors and response to treatment quite reliably in adulthood (Flores et al., 1996). The model involves lesion of the ventral hippocampus (VH) at a critical developmental period in rat pups. The VH is a target for a schizophrenia model because it is forms connections to PFC, NAcc and amygdala but is susceptible to pre- and perinatal stress, including risk factors for schizophrenia and other mental disorders (Tseng et al., 2009). Altered hippocampal volume and shape is seen in first-case – before treatment – and chronic schizophrenia patients, but not in bipolar or schizotypal disorders (Harrison, 2004). Synaptic protein reductions are also observed in the hippocampus, and are related to a patient's cognitive status (Harrison, 2004). Disruptions of spatial and working memory, which involve the VH, are notable symptoms in schizophrenia (Godsil et al., 2013). The neonatal VH (nVH) lesion was established as an animal model of schizophrenia in the early 1990s by B.K. Lipska's group and has demonstrated its relevance to modeling the disorder over two decades (Tseng et al., 2009).

The VH lesion is performed using ibotenic acid on post-natal day 7 (PD7), a timepoint which corresponds with the third trimester in humans (Tseng et al., 2009). The VH has strong connections with the PFC as well as with a number of other cortical and subcortical areas

(Lipska, 2004). Disruption of these emerging and established connections results in a number of behavioural alterations which correspond with symptoms of schizophrenia. Like schizophrenia, nVH lesioned animals appear the same as controls before pubertal maturation (P35), except for some reduced sociability (Flores et al., 2005). The onset of behavioral changes occurs after puberty, and includes impaired reality testing (McDannald et al., 2011); reduced sociability; hyperresponsiveness to stress, dopamine agonists and N-methyl-D-aspartate (NMDA) antagonists (Lipska, 2004); impaired prepulse inhibition (Kamath et al., 2006); and working memory defects (Tseng et al., 2009). This model also shows amelioration of symptoms with traditional neuroleptics, such as glutamate antagonists and haloperidol (Lipska, 2004; Tseng et al., 2009). Interestingly, no changes to PV or GAD67 mRNA levels were seen in the adult PFC after nVH lesion, but cortical excitability was still impaired (Tseng et al., 2008). However, using biased cell counting, which involves extrapolating total neuron numbers from a single sampling site, François et al. (2009) found a reduction in both GAD67+ and PV+ neuron numbers in the PFC of adult rats after nVH lesion, but no reduction in other GABA neuron subtypes. The present project aims to investigate whether neuronal PV or GAD67 protein levels are altered in both adolescent and adult animals, and if there is a subregion-specific alteration to GABA neurons in the PFC, to better characterize cortical interneuron changes in schizophrenia.

Rationale and aim

The present research will focus on GABA neurons in the PFC and Rt. Both these brain regions have higher-order and integrative functions whose disruption could implicate them in schizophrenia, particularly in the production of cognitive symptoms like impaired executive planning and attention. As described above, many proteins related to GABA neuron function are found to be altered in the PFC of schizophrenia patients post-mortem, particularly in

interneurons of the PV+ subtype. Animal models of schizophrenia have also found decreases in GAD67 and PV mRNA and neuron levels in the PFC of adult animals, but no group has looked at total number of neurons expressing these proteins in the PFC before behavioural change and after. The Rt seems highly involved in schizophrenia symptoms and behaviour, yet no study has looked at how it is altered physically or molecularly using an animal model of schizophrenia. Changes to the number of cells expressing GAD67 or PV in this nucleus would alter the overall function of the Rt and would have implications in a number of integrative circuits. Comparing neuron counts before and after behavioural onset for both the PFC and Rt would be valuable for understanding some of the molecular basis of symptom development and progression.

This project aims to determine the total number of GABA neurons (GAD67 positive) and PV-positive neurons in the PFC and Rt using unbiased stereology in a rat model of schizophrenia with a well-established symptomatic behavioural profile, the nVH lesion model (Tseng et al., 2009). To investigate whether changes appear before the onset of schizophrenia-relevant behaviour or after, animals will be sacrificed before puberty (PD20) or in adulthood (PD60). Within the distinct GABA-ergic nucleus of the Rt, cell loss versus cell silencing will be studied by staining for the neuron marker NeuN with PV for orientation.

Hypothesis

It is hypothesized that PV and GAD67 staining will be reduced in both the PFC and Rt in nVH lesion animals, with a greater loss of staining in adulthood, after schizophrenia-relevant behavioural changes, relative to adolescence. These changes in PV and GAD67 expression will provide support for interneuron disruption in schizophrenia through a robust animal model.

Methodology

Animals

Pregnant Sprague-Dawley dams (Charles-River Laboratories) were obtained between embryonic day 17 (E17) and E19 and housed individually to give birth in our animal facility on a 12h light-dark schedule with *ad libitum* access to food and water. On postnatal day 4 (PD4), litters were culled to at most 11 pups with at least 1 female. All experiments were carried out according to the guidelines of the Canadian Council of Animal Care and approved by McGill University Animal Care Committee.

Neonatal ventral hippocampal lesion

On PD7, male pups weighing between 15g and 18g were randomized to sham or lesion groups and anaesthetized with hypothermia in crushed ice (1 min/g body weight). Pups were immobilized to a specially designed plexiglass platform secured to the stereotaxic apparatus by taping them across the shoulders. The skin over the skull was cut from between eyes to behind ears and two holes drilled into the skull to allow the cannula to pass. Lesion animals received an infusion of 0.30µl of ibotenic acid (Sigma; 10 µg/µl in 0.1 M PBS) bilaterally to the VH through a 30-gauge needle attached to a 10µl Hamilton syringe in an infusion pump (coordinates: anterior-posterior -3.0mm from bregma, medio-lateral +/-3.5mm from midline, ventro-dorsal -5.0mm from dura) at a rate of 0.15µl/min, for a total of 2 minutes per side. The cannula was withdrawn 2 minutes after the infusion had ended. The incision was closed using Vetbond™ tissue adhesive (3M™) and ear punching was performed to indicate lesion status. Animals were placed on a heating pad before being returned to their mothers. Sham animals underwent identical operations, but received an infusion of phosphate buffer instead of ibotenic acid.

Perfusion and tissue preparation

To obtain the brains of adolescent animals, half the male pups in each litter were perfused just before weaning on PD20-21. The other half of males in each litter were weaned on PD20-21 and housed two per cage, of alternate lesion status when possible. These weaned animals were perfused in adulthood on PD60.

Animals were anaesthetized with an injection of Ketamine-Xylazine mixture (100 mg/kg Ketamine, 0.8 mg/kg xylazine; 0.1ml cocktail/100g i.p.) and secured to the perfusion table. The chest cavity was opened in a Y shape and a 25⅝ gauge needle attached to the perfusion pump (Harvard Apparatus) was inserted into the left ventricle, then the right atrium punctured with small scissors. Animals were perfused with ice-cold 0.9% saline for 1 minute at a rate of 5ml/min for adolescents and 10ml/min for adults, followed immediately by ice-cold 4% paraformaldehyde (PFA) in 0.1M PBS (1ml/gram body weight). After 15 or 30 minutes for adolescents and adults respectively, perfusion was stopped and brains rapidly removed and fixed in 4% paraformaldehyde at 4°C. After two days, brains were transferred to vials containing 30% sucrose prepared in 0.1M PBS and stored at 4°C. Once the brains sunk to the bottom of the vial (4-5 days), they were wrapped in aluminum foil and frozen on dry ice for 10-15 minutes before being transferred to -80°C for at least overnight.

Brains were sliced into 40µm coronal sections on a cryostat microtome (Leica), from PFC to just before the emergence of the ventral hippocampus (plate 8 to plate 66; Paxinos and Watson, 2005). For each brain, 100-200 sections were collected in a 12-well plate for a total of 6-12 slices per well. Slices were stored free-floating in antifreeze solution at -20°C until further processing.

3,3'-Diaminobenzidine (DAB) chromogen immunohistochemistry

DAB staining was chosen for stereology because it provides a dark, long-lasting stain bound to specific antibodies. Both PV and GAD67 antibodies used provided clear delineation of cell body from background. DAB immunohistochemistry was preferred over immunofluorescence in this study because it is stable over time and will not photobleach under the microscope, which is important for unbiased counting of a large region like the PFC. Since dual staining was not being investigated, DAB immunohistochemistry provided the simplicity and stability desired for this aspect of the experiment.

On the first day of immunohistochemistry, one well of slices was washed in PBS to remove any antifreeze solution, then incubated in hydrogen peroxide (30% (w/w) in H_2O, Sigma) to remove any endogenous peroxidase activity. After washing with PBS again, the slices were incubated for 1 hour at room temperature in a blocking solution of 5% normal horse serum (Sigma) and 0.5% Triton-X (Sigma) prepared in PBS. Slices were then transferred directly to blocking solution containing primary antibodies against either PV (1:4000; mouse monoclonal; Sigma) or GAD67 (1:1000; mouse monoclonal; Sigma) for 2 hours at room temperature then at 4°C overnight. Negative controls were run by adding slices to blocking solution without primary antibody.

On the second day, slices were washed in PBS then incubated for 2 hours in blocking solution containing biotinylated anti-mouse secondary antibody raised in horse (1:250; Vector). They were washed in PBS again before incubating in avidin/biotin Vectastain© ABC Kit (standard; Vector) for 30-40 minutes, followed by a final PBS rinse. Slices were developed using 3,3'-Diaminobenzidine (DAB) peroxidase plus nickel kit (Vector) and reaction was stopped by

transferring slices to PBS. Slices were mounted in anterior to posterior order onto charged microscope slides (Snowcoat X-tra; Leica) using PBS and let dry overnight. The following day slides were dehydrated in increasing concentrations of ethanol followed by xylene and coverslipped with Permount (Thermo Fisher Scientific).

Immunofluorescence

The immunofluorescence technique was used to investigate the presence of two different proteins in the same cell. It is not possible to do this with DAB immunohistochemistry and the proteins of interest. The images produced also provide a high contrast for comparison of single and dual stained cells.

The first day of immunofluorescence followed the same protocol as DAB staining, except no hydrogen peroxide wash was applied and thus only one PBS wash was used before incubating in blocking solution. The primary antibodies used were anti-NeuN (1:300, rabbit monoclonal; Millipore) and anti-PV (1:4000, mouse monoclonal; Sigma) in a blocking solution of 0.5% PBS-T with 10% donkey serum.

On the second day, slices were washed in PBS then incubated in the dark at room temperature for 2 hours in blocking solution with Alexa Fluor® 546-conjugated donkey anti-rabbit (1:300, red; Fisher Scientific) and Alexa Fluor® 488-conjugated donkey anti-mouse (1:1000, green; Fisher Scientific) antibodies. Slices were washed again with PBS, mounted on charged slides and left to dry in the dark for 2 hours. Once dry, slides were coverslipped with VECTASHIELD® mounting medium containing DAPI (Vector) and stored flat in the dark at 4°C until imaging.

Lesion verification

Coronal slices of the VH were taken at 30µm thickness on a cryostat immediately after tissue collection for immunohistochemistry. Starting just before appearance of the ventral hippocampus (plate 67; Paxinos and Watson, 2005), every fifth slice was collected directly onto a microscope slide until the hippocampus ended. Sections were stored at -80°C for at least one night overnight before staining with 0.5% cresyl violet (Sigma). Briefly, slides were brought to room temperature, then washed in progressively decreasing concentrations of ethanol before incubating in 1x PBS for 10 minutes followed by cresyl violet for 30 seconds. Slides were dehydrated in increasing concentrations of ethanol followed by a bath of Xylene (Fischer) and coverslipped with Permount (Fischer). Accepted lesions were those slices showing bilateral neuron loss, cavitation and/or retraction in the area of the VH with the dorsal hippocampus and surrounding brain structures preserved, and visualized at 1x magnification using the MCID Image Analyser.

Estimation of total neuron count in PFC and Rt

The total number of PV neurons in the PFC or Rt were estimated using unbiased stereology through Stereoinvestigator® software (Microbrightfield Inc) and a Zeiss Axio Imager.M1 microscope with motorized stage, attached to a Hamamatsu Orca-ER camera. The outline of the area of interest was drawn on each section (1-in-4 series, each 120µm apart from each other; eight sections for PFC and twelve sections for Rt per rat). In the case of NeuN-PV dual staining, PV staining was used to locate and trace the Rt, then only NeuN+ cells were counted. Within the PFC, separate outlines were made for the infralimbic, prelimbic and

cingulate cortex, and right and left sides were counted as separate data points for both the PFC and the Rt.

For the PFC, a sampling grid of 150 x 150 μm was overlayed on the section and a 70 x 70μm counting frame was used at each *x-y* step. For the Rt, a 140 x 140μm grid with a 50 x 50μm counting frame was used. Counting was performed with a 12μm dissector thickness and a 4μm guard height to prevent counting of neurons located on the top or bottom of the section.

Statistics

Statistical analysis was done with Rochford Statistics programs. For neuronal PV and GAD67 expression counts in the PFC, total neuron counts were analysed with a two-way between ANOVA for lesion status and age. The PFC was broken down using a two-way mixed ANOVA with PFC subregion as the within factor and lesion status as the between factor, at the two age points. A simple main effects test of lesion versus sham numbers for each brain region was done to identify which region(s) in particular varied significantly. In the Rt, a two-way between ANOVA was performed for lesion status and age of perfusion, separately for both PV and GAD67 neuron counts. A two-way mixed ANOVA was performed to compare NeuN and PV counts in the Rt, with lesion status as the between factor and stain as the within factor.

Results

Lesion

Lesions performed on PD7 had a 73% success rate for this experimental cohort (4 unsuccessful out of 15 lesions performed with ibotenic acid). The right-hand image in figure 1 represents the typical bilateral neuron loss, cavitation and/or retraction in the area of the VH,

with the dorsal hippocampus and surrounding brain structures preserved, which was considered a successful lesion.

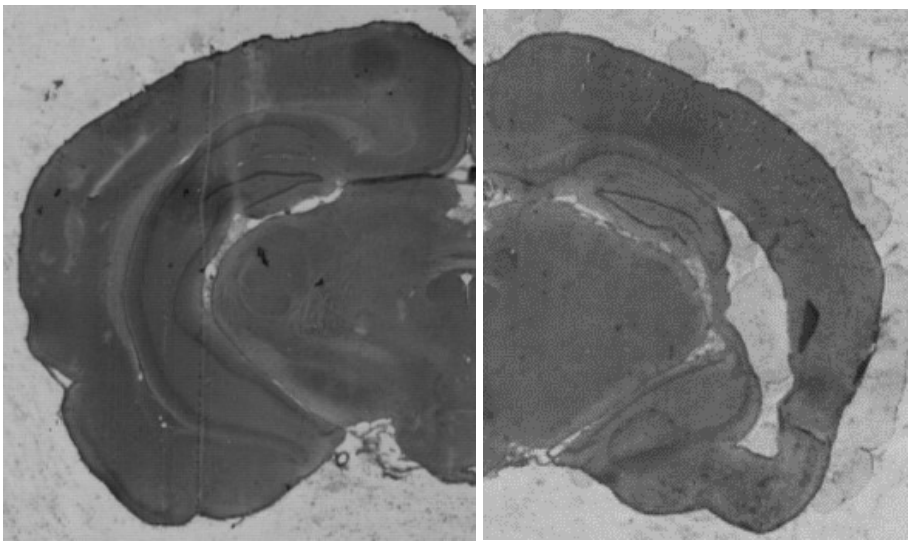

Figure 1. A representative image of nVH lesion. A Cresyl violet stain showing the comparison of ventral hippocampus in sham (PBS injected, left) and lesion (ibotenic acid injected, right) animals at PD60.

PFC neuron counts

The total number of neurons expressing PV and GAD67 in the PFC were estimated using unbiased stereology. Figure 2 shows the typical DAB staining of PV+ and GAD67+ neurons in the PFC, as seen while counting cell bodies at 40x magnification. When tracing, the PFC was separated into three subregions: the cingulate, prelimbic and infralimbic cortices. Figure 1a in the appendix represents a typical tracing of the subregions in the PFC in Stereoinvestigator, using the Rat Brain Atlas as a guide (plate 11; Paxinos and Watson, 2005).

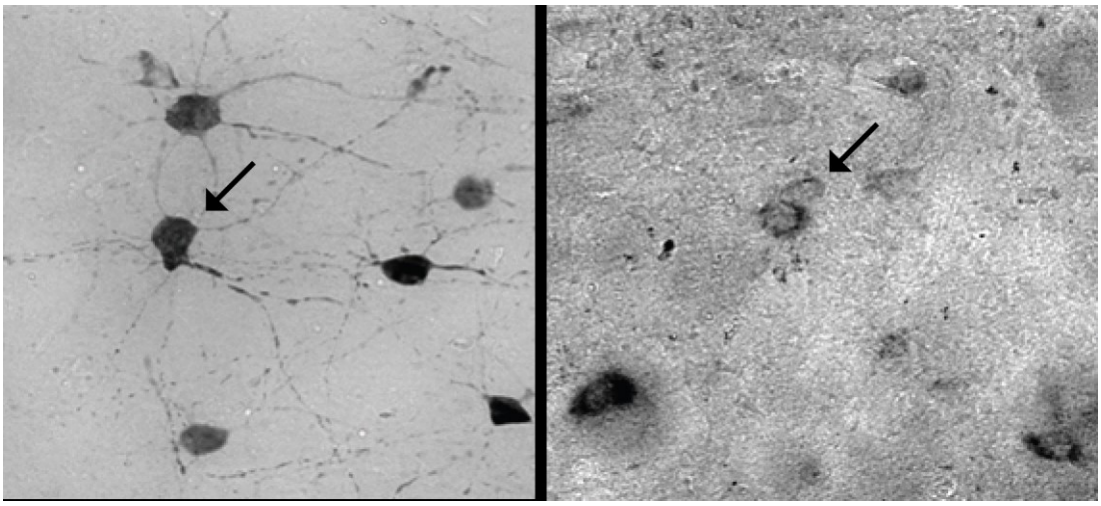

Figure 2. Representative DAB staining in the adult (PD60) PFC for PV (left) and GAD67 (right). Arrows are pointing to a typical cell body that would be counted during stereology. 40x magnification.

Table 1 and 2 in the appendix show the raw counts for PV and GAD67 respectively, at both age points. These counts were performed on 4 sham and 4 lesion animals per age group, for a total of 16 animals. For the PFC, total counts were calculated using 8 brain sections per animal, each section 40μm thick and 120μm apart from the next. Two groups of 8 sections were used per animal – one group for PV+ counts and one for GAD67+ counts. Counts from single sections were lateralized into right and left and each side was used as a separate data point, for a total of 16 data points per animal per stain. The total number of PV+ or GAD67+ neurons for all regions combined was calculated, then separated by subregion. Each region forms connections with different subcortical areas, and differences in PV or GAD67 expression levels in only one of the subregions may suggest disruption of particular connections or subcortical areas (Godsil et al., 2013).

Analyzing PV+ counts, a two-way between ANOVA, comparing age of perfusion and lesion status, yielded no significant age by lesion status interaction ($F(1,28)=1.56$, $p>0.22$; figure

3). However, there were significantly fewer PV+ neurons at PD20 than PD60, suggesting that PV+ neurons have not reached adult levels at PD20 ($F(1,28)=11.52$, $p<0.0021$).

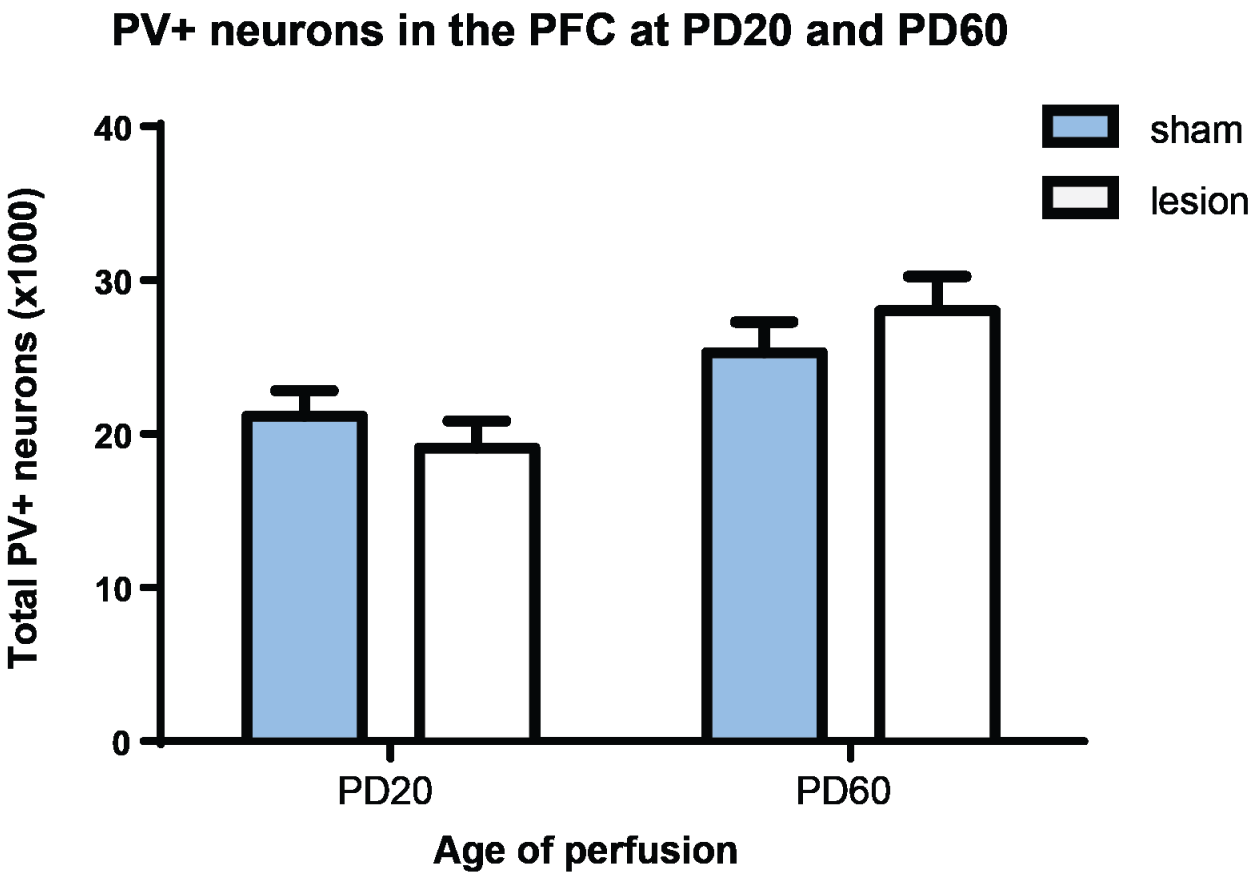

Figure 3. Total number of PV+ neurons in the PFC in sham and lesion animals at PD20 (adolescence; n=4,4) and PD60 (adulthood; n=4,4). There is no significant difference in total neuron numbers between sham and lesion animals in either age group, $F(1,28)=1.56$, $p>0.22$.

The PFC was then divided into the three subregions – cingulate, prelimbic and infralimbic – and PV+ neurons in these subregions were analyzed at PD20 or PD60, as illustrated in figures 4 and 5 respectively. This was done using a two-way mixed ANOVA, with lesion status as the between factor and PFC subregion as the within factor. When lesion status was compared within each subregion, a simple main effects test showed no significant difference between total PV+ neuron counts in sham and lesion animals at PD20 ($Fs(1,23)\leq1.38$, $ps>0.25$) nor PD60 ($Fs(1,23)\leq1.34$, $ps>0.26$) in the PFC.

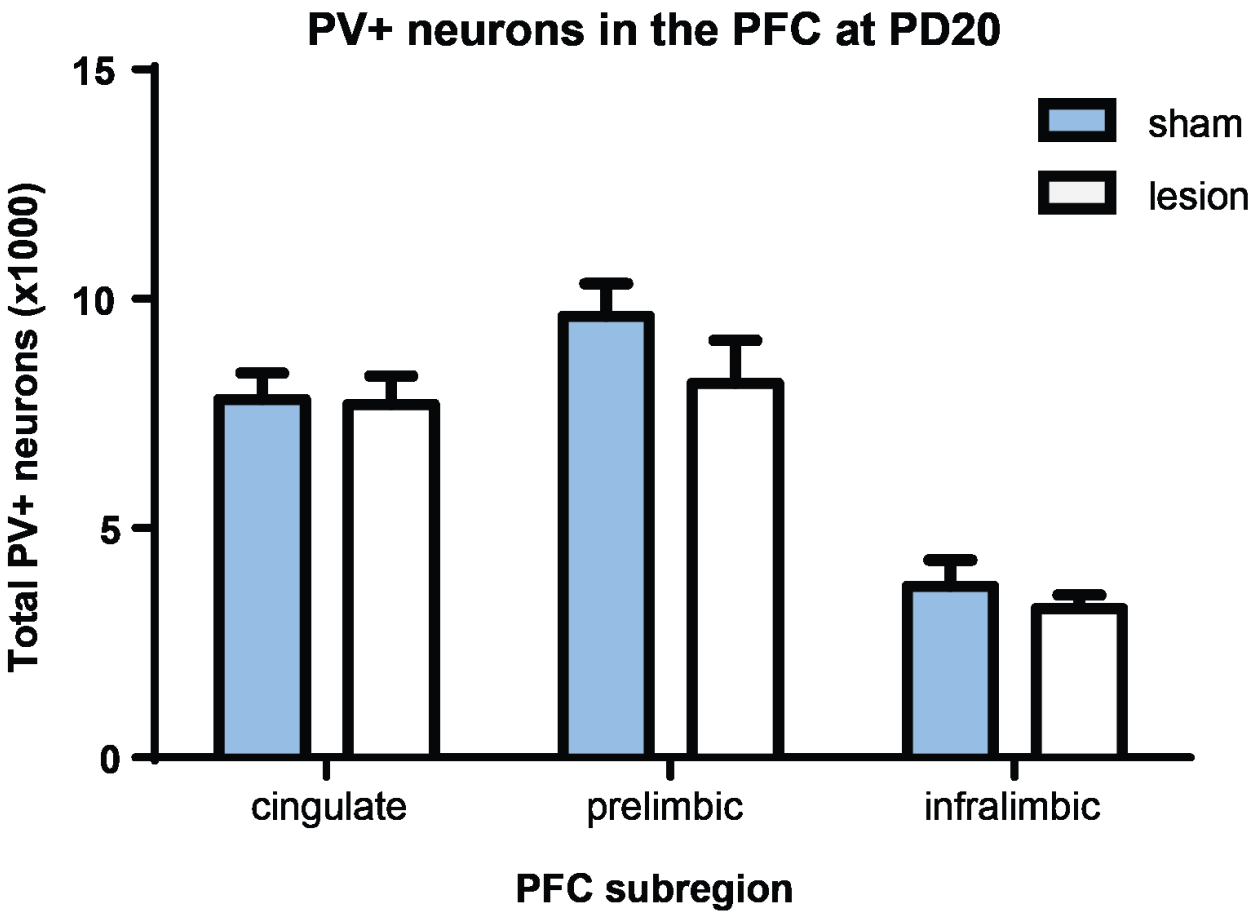

Figure 4. Total number of PV+ neurons in the PFC subregions (infralimbic, prelimbic and cingulate) in sham (n=4) and lesion (n=4) animals at PD20 (adolescence). No significant difference is found in total neuron numbers between sham and lesion animals in any subregion at this age, $Fs(1,23) \leq 1.38$, $ps > 0.25$.

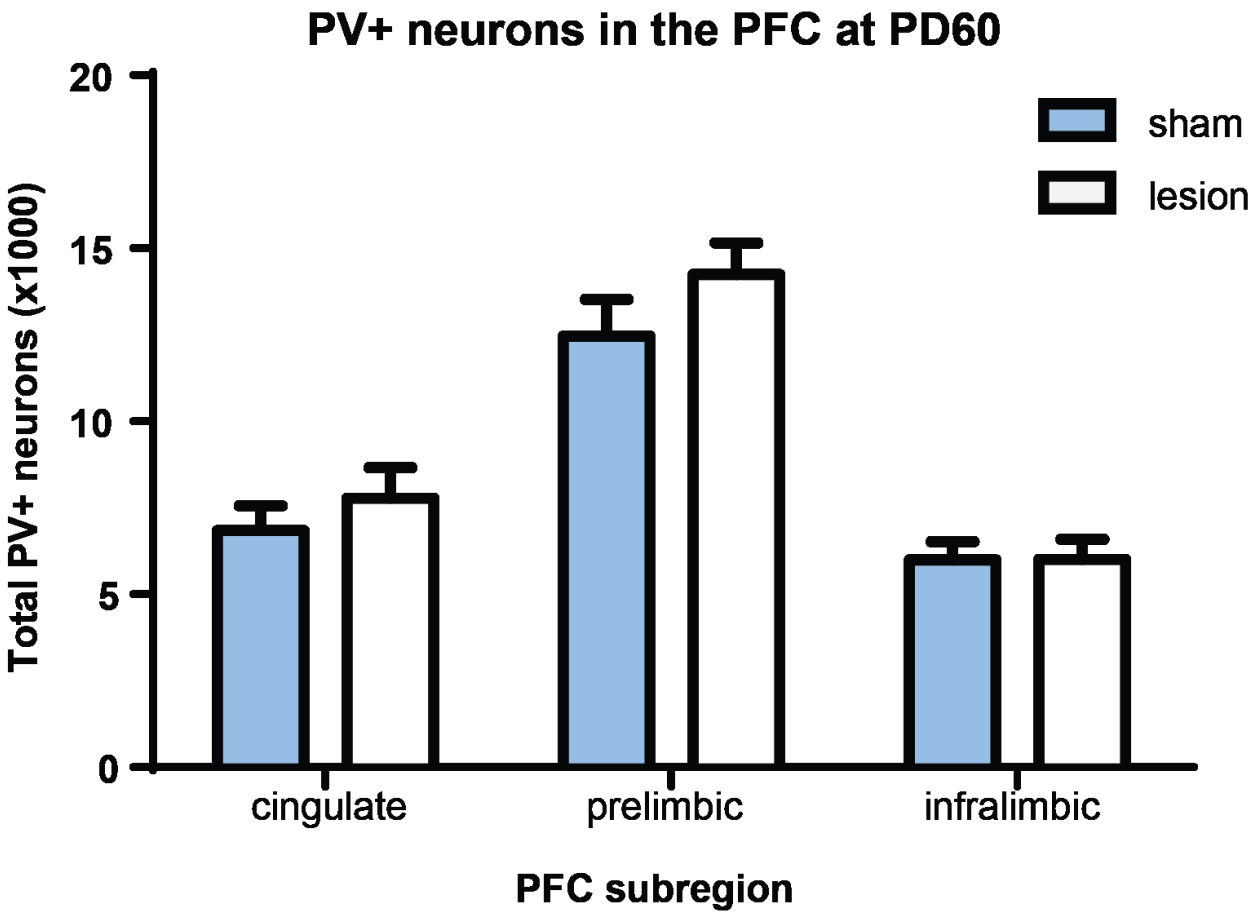

Figure 5. Total number of PV+ neurons in the PFC subregions (infralimbic, prelimbic and cingulate) in sham (n=4) and lesion (n=4) animals at PD60 (adulthood). No significant difference is found in total neuron numbers between sham and lesion animals in any subregion at this age, $Fs(1,23) \leq 1.34$, $ps > 0.26$.

GAD67+ counts were analyzed in the same way as the PV+ counts described above, with 4 animals per group and 8 sections per animal, lateralized into 16 data points per animal. Like PV+ neurons, there was no significant age by lesion interaction found for total GAD67+ neurons in sham and lesion animals across the whole PFC (two-way between ANOVA, $F(1,28)=1.51$, $p>0.22$; figure 6). There was also no significant difference between total neuron counts at PD20 and PD60, suggesting that GAD67+ neuron numbers have reached adult levels by PD20 ($F(1,28)=1.77$, $p>0.19$).

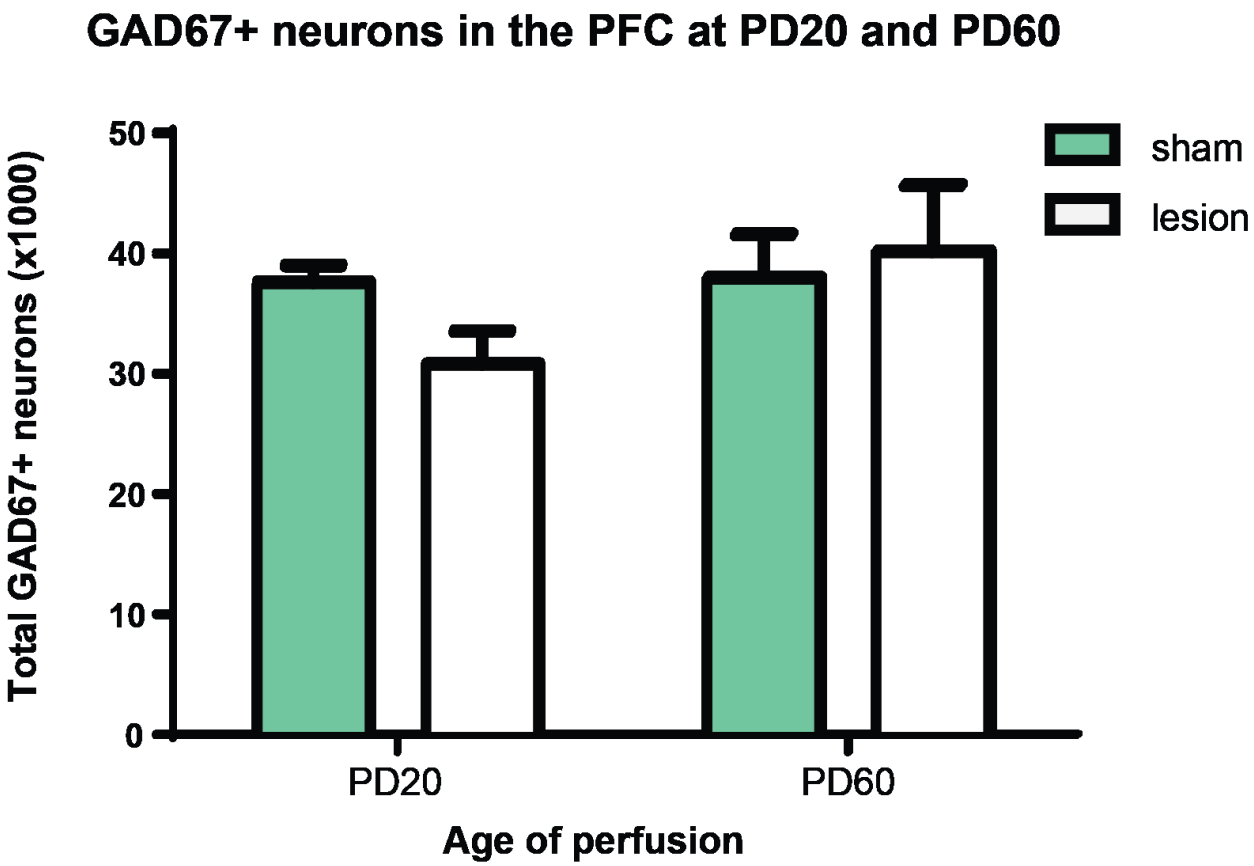

Figure 6. Total number of GAD67+ neurons in the PFC in sham and lesion animals at PD20 (adolescence; n=4,4) and PD60 (adulthood; n=4,4). There is no significant difference in total neuron numbers between sham and lesion animals in either age group, $F(1,28)=1.51$, $p>0.22$.

Once again, the PFC was separated into the three subregions of cingulate, prelimbic and infralimbic areas, and GAD67+ neuron numbers were analyzed using a two-way mixed ANOVA (subregion as within and lesion status as between factor) at both PD20 and PD60. At PD20 there was a significant lesion status by subregion interaction found, meaning there was a significant difference in total neuron counts between the subregions in both sham and lesion animals ($F(2,28)=4.46$, $p<0.02$). This is expected but uninformative because, as seen in figure 1a, the subregions themselves vary in size, and a larger subregion will contain significantly more neurons when neuron distribution is consistent overall. However, as seen in figure 7, a simple main effects test of lesion status at subregion revealed a significant reduction in GAD67+

neurons in only the prelimbic area of lesion animals at PD20 ($F(1,27)=6.86$, $p<0.015$). The cingulate and infralimbic regions at this age had $Fs(1,27)\leq 2.08$, giving $ps<0.16$. By PD60, the simple main effects test of lesion status at subregion showed no difference in GAD67+ neuron numbers between sham and lesion animals in any of the three PFC subregions ($Fs\leq 0.15$, $p>0.70$; figure 8).

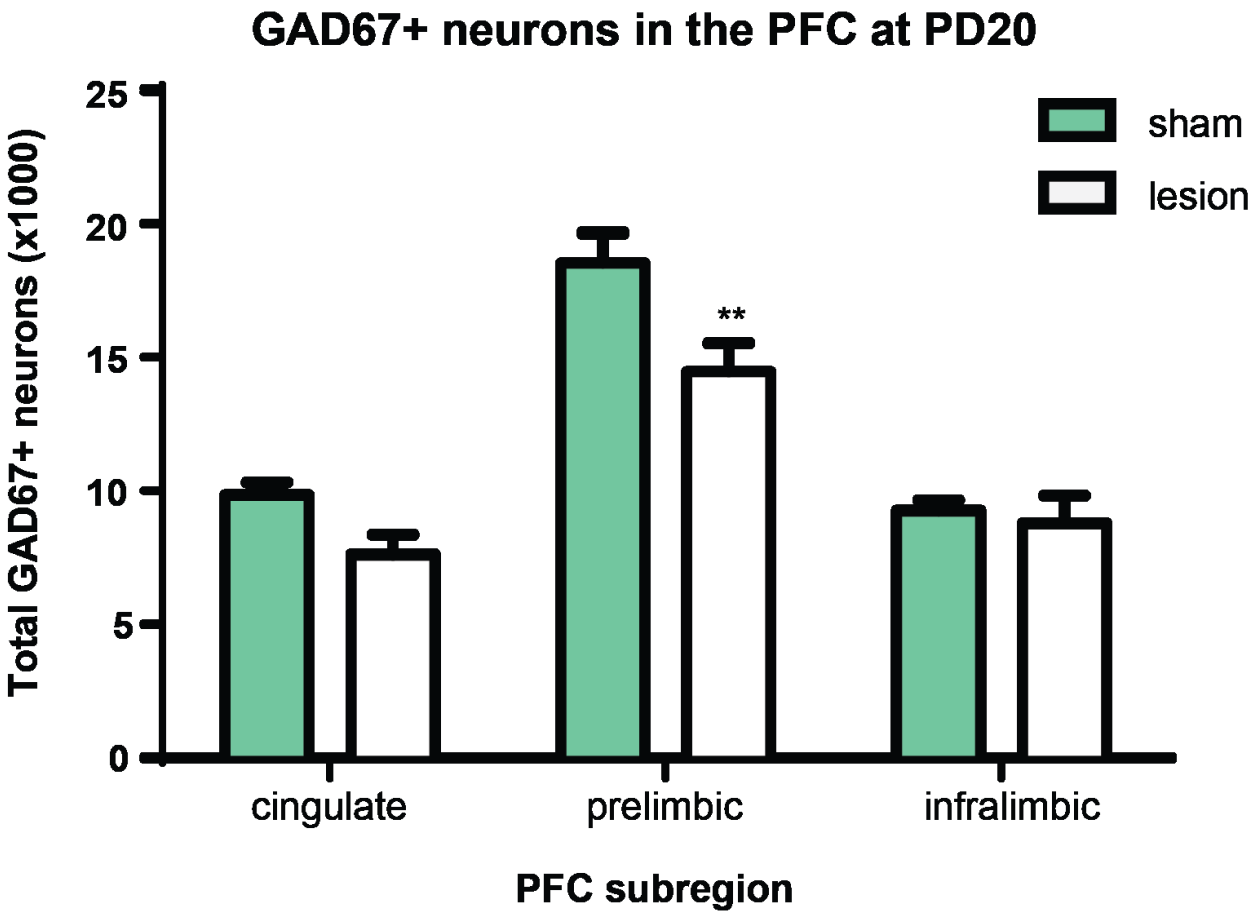

Figure 7. Total number of GAD67+ neurons in the PFC subregions (infralimbic, prelimbic and cingulate) in sham (n=4) and lesion (n=4) animals at PD20 (adolescence). There is a significant reduction in GAD67+ neurons in the prelimbic area of lesion animals at this age. **p>0.015

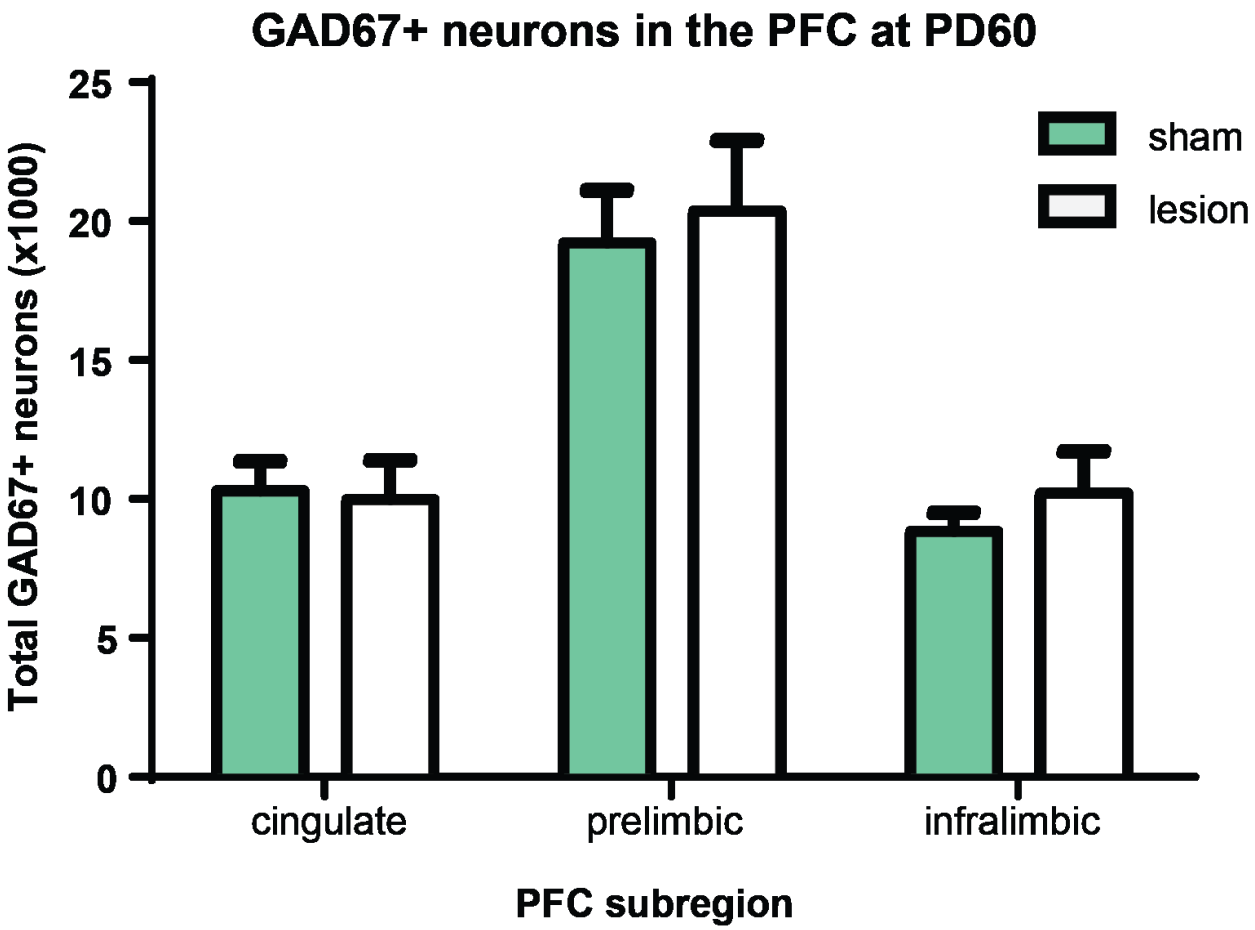

Figure 8. Total number of PV+ neurons in the PFC subregions (infralimbic, prelimbic and cingulate) in sham (n=4) and lesion (n=4) animals at PD60 (adulthood). No significant difference is found in total neuron numbers between sham and lesion animals in any subregion at this age, Fs≤0.15, ps>0.70.

Rt structure and neuron counts

There was a notable visible change in the shape of the Rt in both PD20 and PD60 animals, even before performing any neuron count analysis. As seen in figure 9, the dark PV staining shows the distinct "C" shape of the nucleus in sham animals. However, staining is almost completely absent in the lesion animals, particularly in the curved side of the C as the slices progress caudally. The top and tail of the nucleus were often conserved in the lesion animals. Although figure 9 only shows consecutive coronal slices at PD20, the same loss-of-staining pattern was seen in PD60 animals. Whether this loss of PV expression is a result of cell

loss or simply reduced PV expression is investigated using NeuN-PV dual fluorescence in the next section.

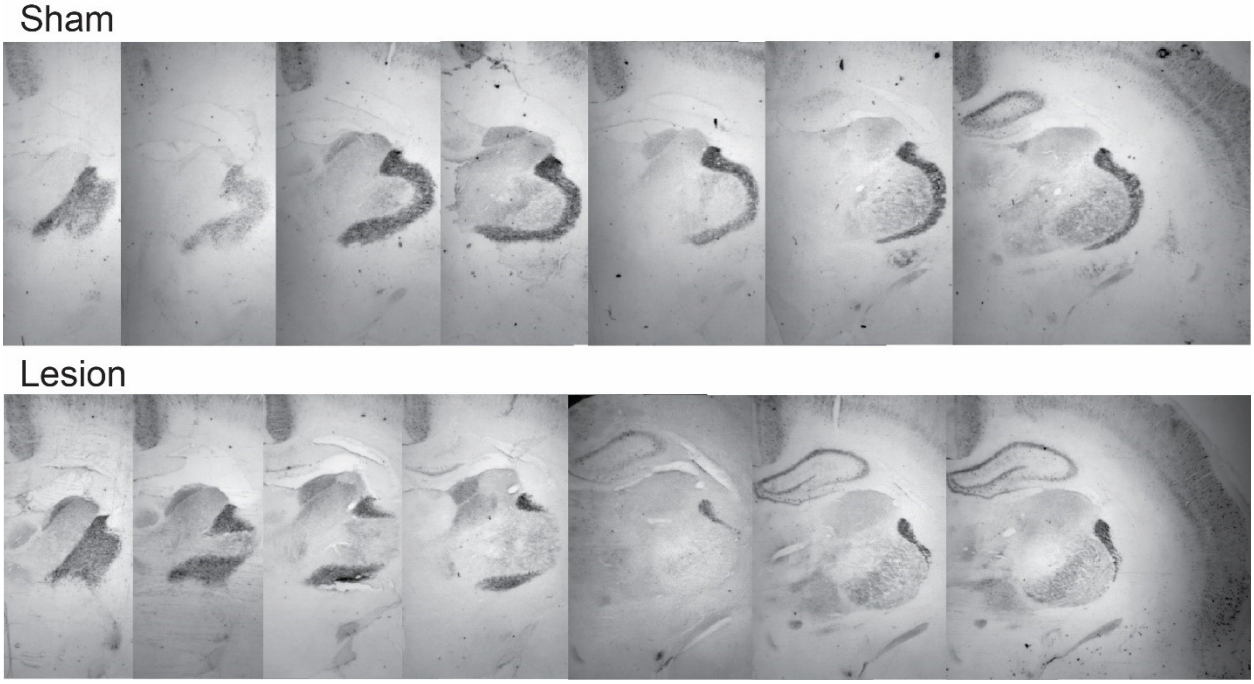

Fig 9. 1x images of DAB-stained PV+ cells in the Rt of sham (top) and lesion (bottom) animals at PD20. These 7 consecutive coronal sections are 120µm apart and progress rostrally to caudally moving left to right. The Rt is darkly stained and centred in each image, and the dorsal hippocampus emerges on the top of the more caudal images.

Total PV+ or GAD67+ neuron numbers were investigated using unbiased stereology. These counts were performed on 4 sham and 4 lesion animals per age group, for a total of 16 animals. For the Rt, total counts were calculated using 12 brain sections per animal, where each section was 40µm thick and 120µm apart from the next. Two groups of 12 sections were used from the same animal: one group stained for PV and one for GAD67. Counts from the left and right Rt nuclei of the same animal were included as separate data points for a total of 24 data points per animal per stain. Table 3 and 4 of the appendix show the raw counts for PV+ and GAD67+ neurons respectively.

Total neuron counts were analyzed using a two-way between ANOVA comparing age and lesion status. For PV+ neuron counts, a significant age by lesion status interaction was found ($F(1,28)=9.21$, $p<0.0052$). As seen in figure 10, breaking this interaction down with a simple main effects test revealed a dramatic reduction in the number of PV+ neurons in lesion animals at both PD20 ($F(1,28)=24.84$, $p<0.00003$) and PD60 ($F(1,28)=86.04$, $p<0.00001$).

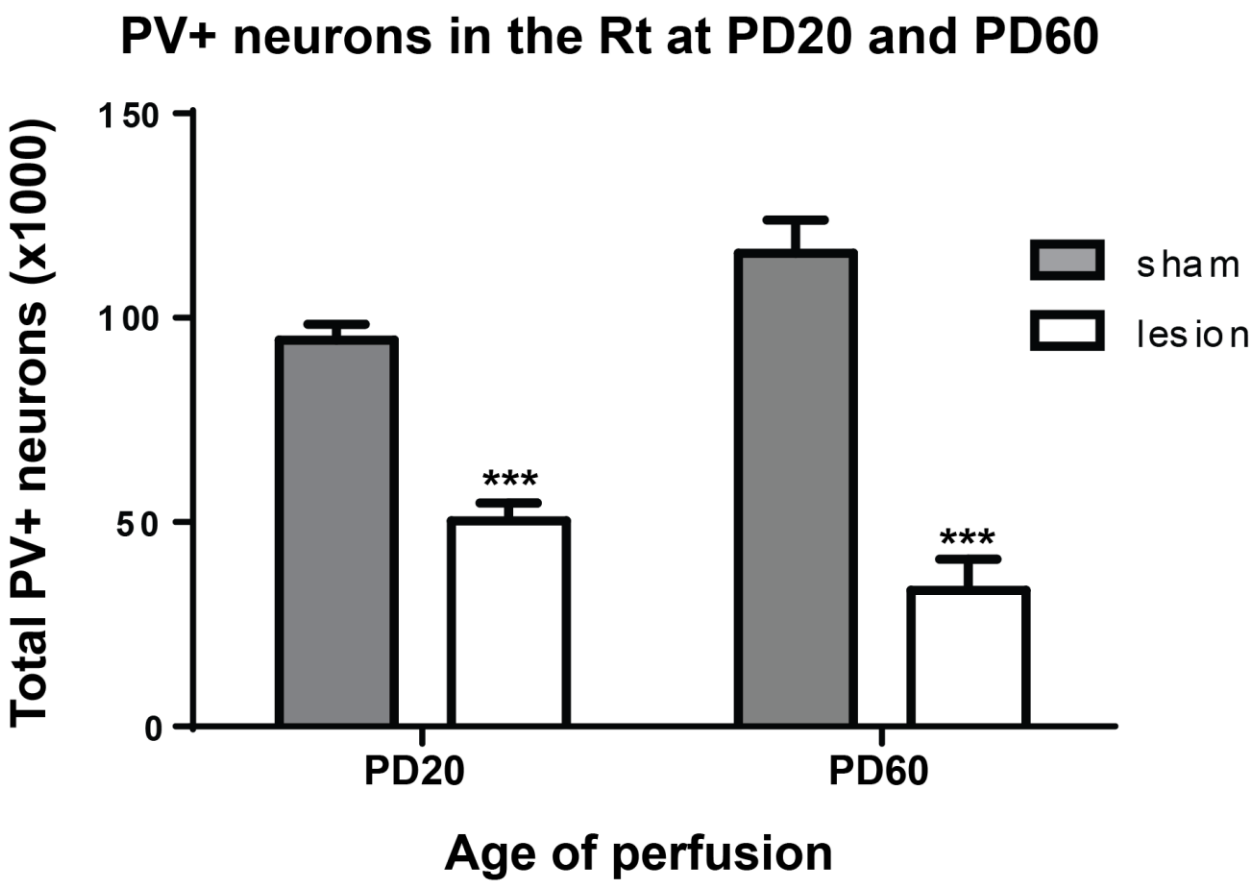

Figure 10. Total number of PV+ neurons in the Rt in sham (n=4) and lesion (n=4) animals at PD20 (adolescence; n=8) and PD60 (adulthood; n=8). A significant reduction in PV+ neuron numbers is found in lesion animals at both PD20 and PD60. ***p<0.00003.

The same analysis described above for PV+ neuron counts was performed on GAD67+ counts. A two-way between ANOVA for age and lesion status gave no significant age by lesion interaction, which is expected when the neuron counts for the two ages do not differ greatly. Using a simple main effects test to compare the sham and lesion counts at each age point

revealed a significant reduction in GAD67+ neurons in lesion animals at PD20 ($F(1,28)=19.59$, $p<0.00013$) and PD60 ($F(1,28)=39.83$, $p<0.00001$), as shown in figure 11.

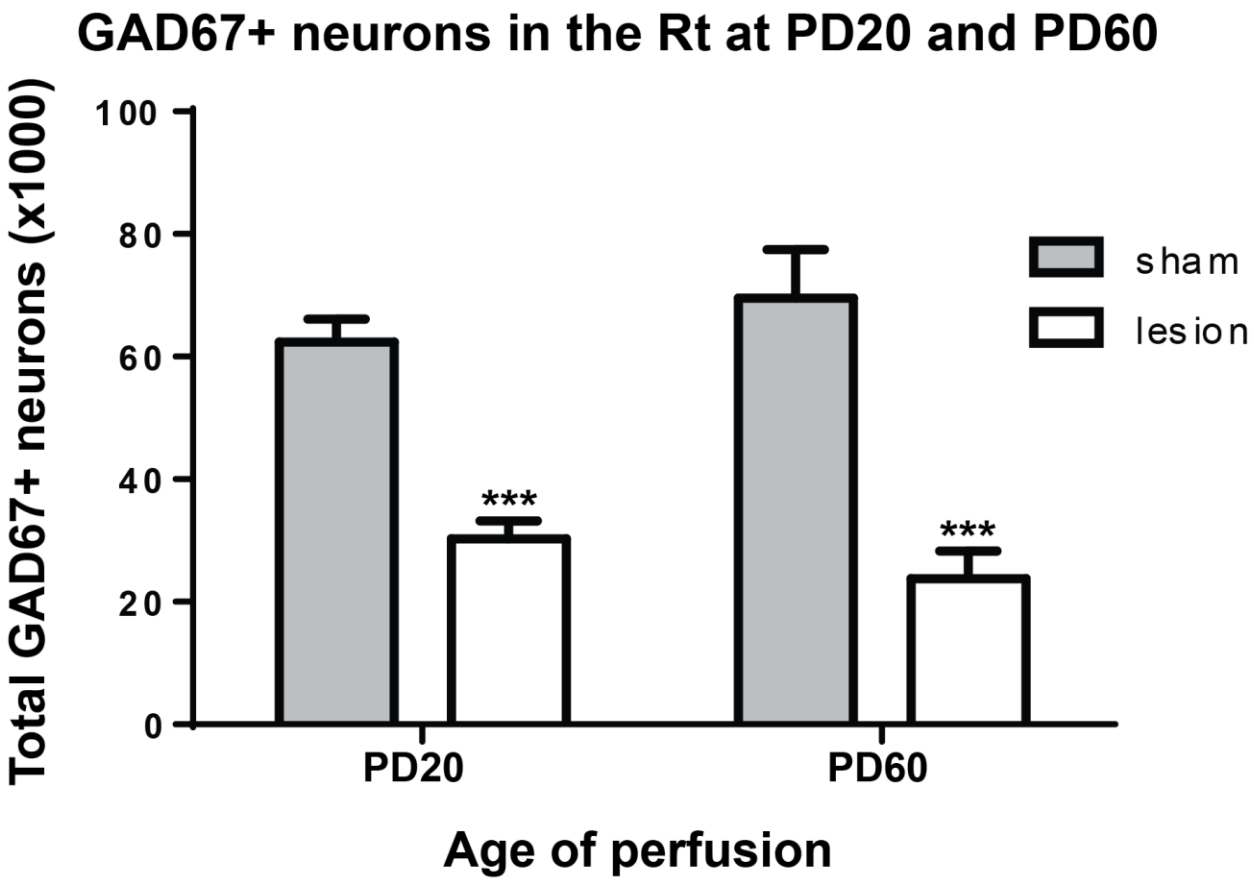

Figure 11. Total number of GAD67+ neurons in the Rt in sham (n=4) and lesion (n=4) animals at PD20 (adolescence; n=8) and PD60 (adulthood; n=8). A significant reduction in PV+ neuron numbers is found in lesion animals at both age points. ***p<0.00013.

NeuN-PV fluorescence in the Rt

In order to investigate whether loss of PV and GAD67 expression in the Rt reflected neuronal loss, slices from 2 lesion and 2 sham animals per age group were stained with the neuronal marker NeuN along with PV to allow accurate location of the Rt. As seen in figure 12 and 13, the morphology of cells stained with NeuN in sham animals is rounder and smaller than the surrounding thalamic nuclei, which helps distinguish the Rt when PV staining is not present.

Also visible in these figures is the presence of dual staining between NeuN and PV in both sham and lesion animals, as well as the lack of NeuN staining in the Rt of lesion animals at both ages. Although it is not investigated in this study, it is interesting to note that the staining of PV+ processes in the inner thalamic nuclei, to which the Rt projects widely, does not appear greatly reduced.

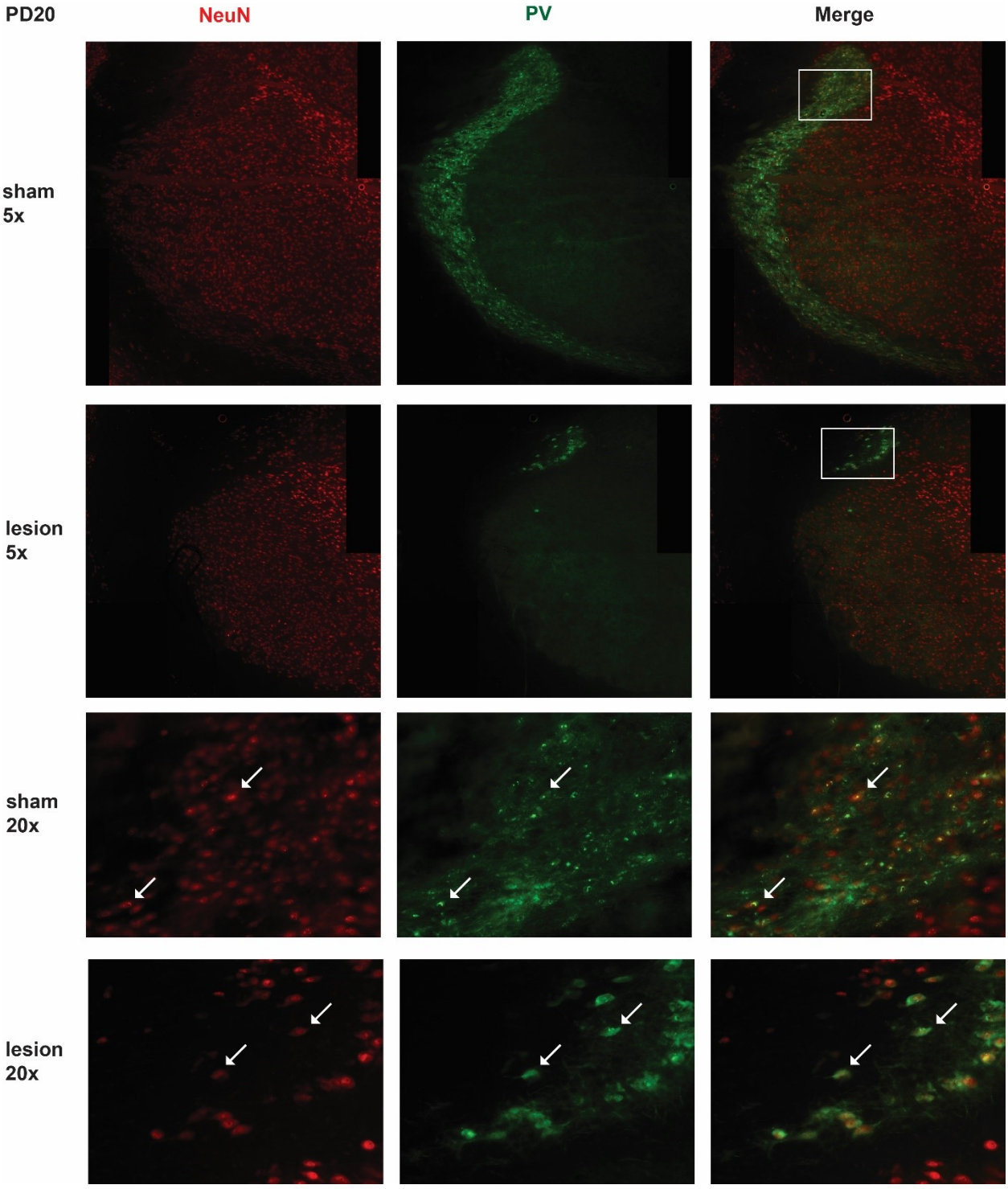

Figure 12. Fluorescent staining for PV and NeuN in the Rt of a sham and lesion animal at PD20. 5x magnification (top) shows the gross loss of NeuN staining in the lesion animals, with the white rectangle outlining the area magnified to 20x (bottom). 20x magnification shows more detail of the dual staining for PV and NeuN, with arrows pointing to example dual-stained neurons.

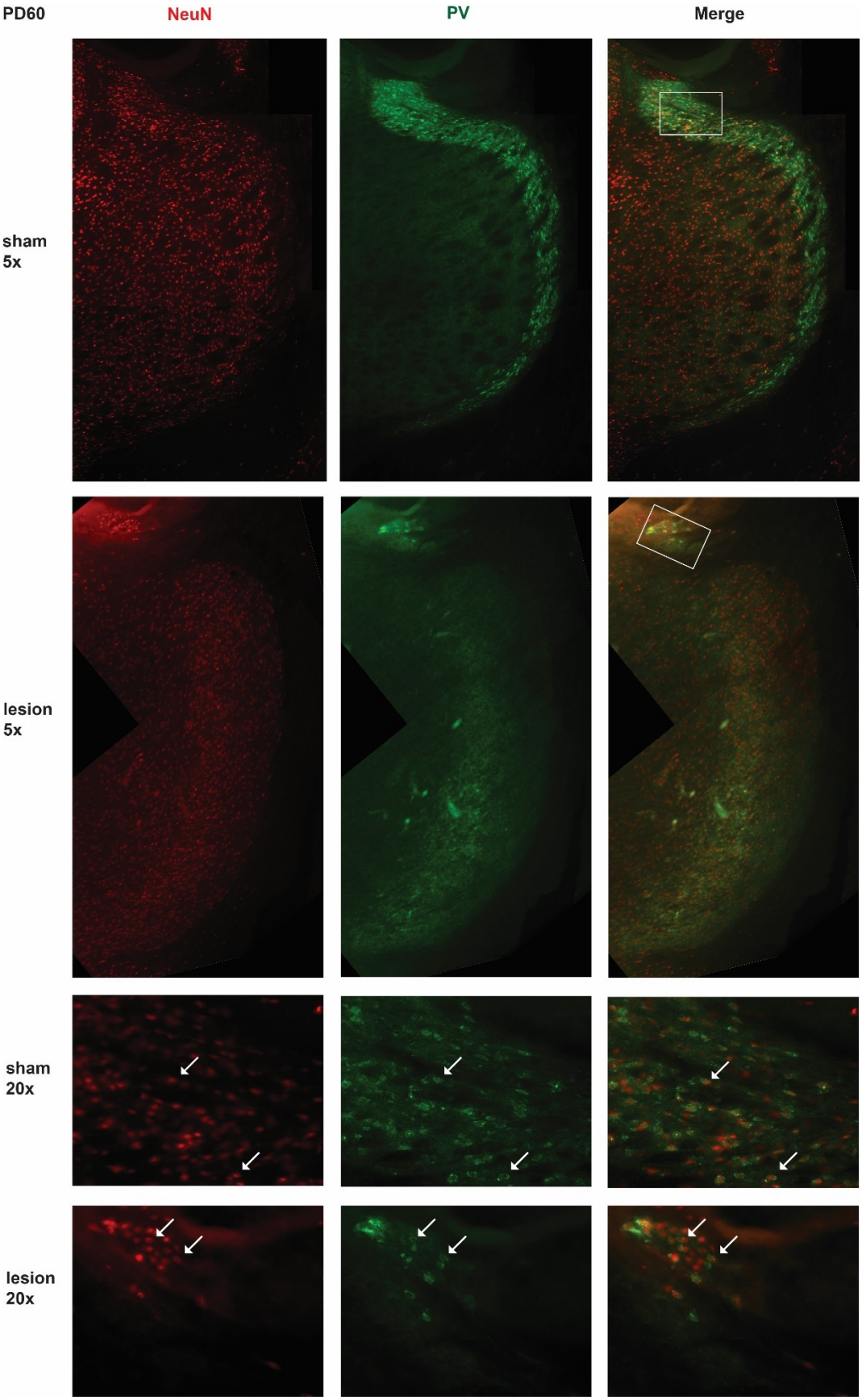
PD60
NeuN
PV
Merge
sham
5x
lesion
5x
sham
20x
lesion
20x

Figure 13. Fluorescent staining for PV and NeuN in the Rt of a PD60 sham and lesion animal. 5x magnification shows the gross loss of NeuN staining in the lesion animals, with the white rectangle outlining which area is magnified to 20x. 20x magnification shows more detail of the dual staining for PV and NeuN, with arrows pointing to example dual-stained neurons.

Exploratory stereology was performed on the small sample of slices that were dual-stained for NeuN and PV to get an idea of how NeuN+ and PV+ neuron counts compare. There was a total of 2 sham and 2 lesion animals stained and counted at each age, for a total of 8 animals counted. Once again, the right and left nuclei from the same animal were counted as separate data points, for a total of 16 data points. Table 5 of the appendix shows the raw counts for NeuN+ neurons in the Rt.

NeuN+ cell bodies were counted alone and the totals were then compared to the previous PV+ counts obtained from DAB staining. If there is a loss of cells along with the loss of PV expression, there should be no difference between PV and NeuN counts in the Rt. Given the large difference already found between total neuron counts in sham and lesion animals (figure 10), variability in the samples was reduced by performing a two-way mixed ANOVA with stain as the within factor and lesion status as the between factor, ignoring age by grouping both PD20 and PD60 data points under the lesion status variable.

Figure 14 shows the results of this analysis. No significant lesion status by stain interaction was found ($F(1,14)=0.14$, $p>0.70$). Performing a simple effects test also showed no significant difference between NeuN and PV counts in either sham or lesion animals ($Fs(1,14)\leq 0.15$, $ps>0.70$).

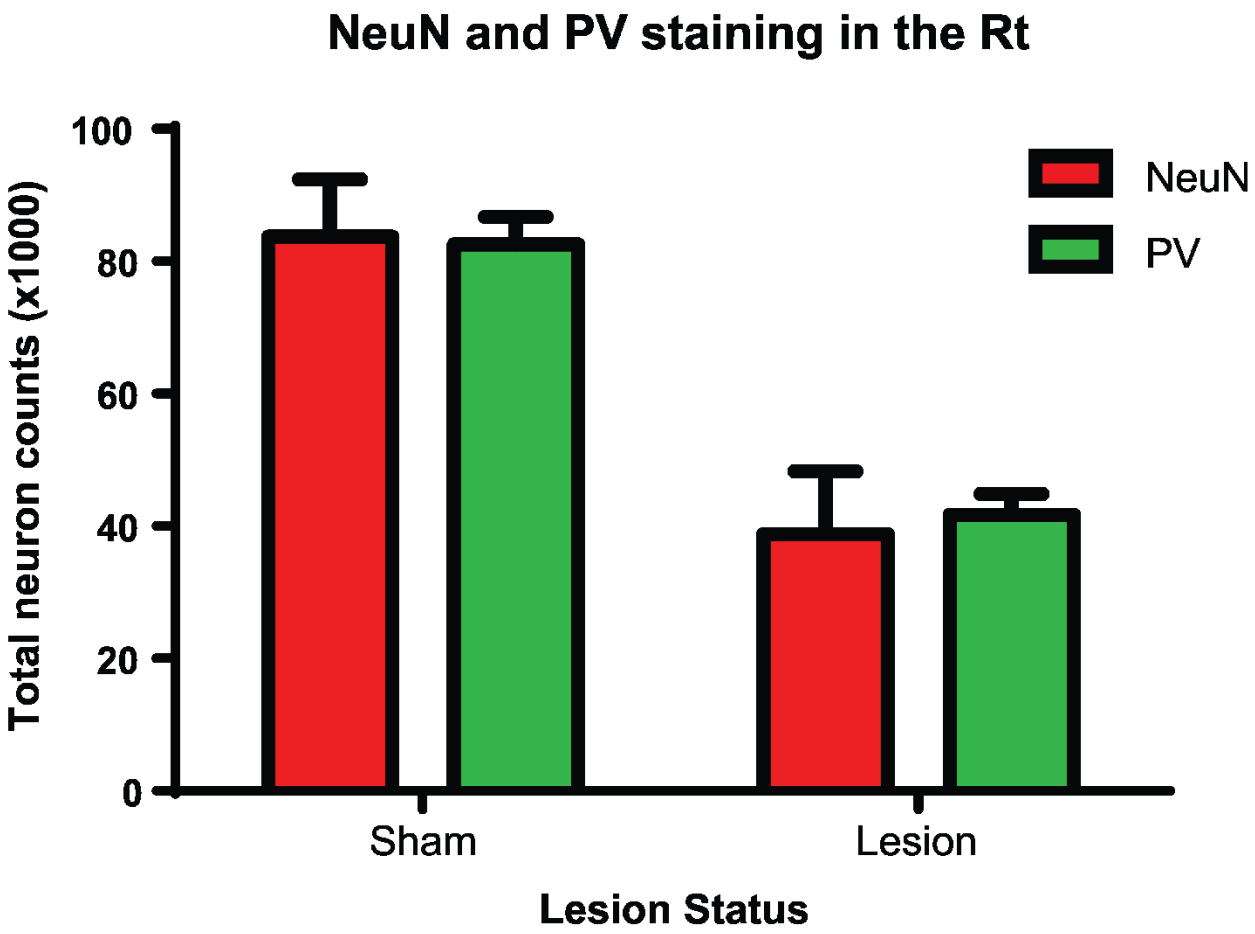

Figure 14. Neuronal marker NeuN and PV staining in the Rt in sham (n=4) and lesion (n=4) animals. No significant difference was found between NeuN+ and PV+ neuron numbers in sham or lesion animals, Fs(1,14)≤0.15, ps>0.70.

Discussion

Prefrontal Cortex

In both adolescence and adulthood, this study found no significant difference in total PV+ neuron counts across the PFC between sham and lesion animals. When the PFC was divided into functional subregions, there was still no apparent reduction in PV+ neurons at PD20 or PD60 in lesion animals. This is not in accordance with the hypothesis that there would be fewer PV+ neurons in the PFC of animals showing a schizophrenia-related behavioural phenotype. However, a low n of 4 per group may have hindered any small but significant findings.

Additionally, this study did not compare relative counts of PV+ basket and chandelier cells. Basket and chandelier cells are both fast-spiking, but basket cells synapse on the dendrites and soma, while chandelier cells synapse at the axon hillock (Gonzales-Burgos et al., 2011). There are some studies which suggest GABA released from chandelier cells onto the axon hillock is excitatory, and that PV+ basket cells are the cell type that generate gamma rhythms (Curley and Lewis, 2012). Thus, one cell type may be affected without changing the overall neuron number, while still producing distinct behavioural changes.

Although no reduction in PV+ neurons was seen, GABA functionality is known to be impaired by other means. In nVH lesion animals in particular, GAD67 mRNA in the PFC is reduced in adult rats (Lipska and Weinberger, 2000). There is also a decrease in $GABA_A$ receptor mRNA in the PFC at adolescence, yet an increase in adulthood (Endo et al., 2007). This increase in receptors may be in compensation for lower GABA production. There are also alterations to the dopamine and glutamate systems, which interact with the inhibitory system and are also implicated in schizophrenia. Bitanihirwe in 2009 found that NMDA receptor 2A is reduced on PV+ neurons exclusively, associated with a decrease in excitatory presynaptic densities at these neurons in the PFC of post-mortem human brains. This reduction in excitatory signalling in turn decreases the synthesis and release of GABA in these neurons (Nakazawa et al., 2012). These NMDA receptor changes may also result in dysregulation of cortical synchrony and altered gamma band power in the PFC (Nakazawa et al., 2012), although gamma band synchrony hasn't been investigated using the nVH lesion model.

Notably, GAD67+ neurons were reduced in the prelimbic region of the PFC at PD20 but not PD60. The prelimbic area connects reciprocally to a number of limbic areas as well as the nucleus reuniens and subiculum of the hippocampus. It is involved in action-outcome detection,

working memory, and anxiety and stress (Dalley et al., 2004). The loss of inhibitory interneurons in this region before symptom onset but not after may reflect a delay in developing a GAD67+ profile in these neurons. This, in turn, could affect migration and integration of recently born neurons, due to GABA's role in guiding developing cortical neurons (Jovanovic and Thompson, 2011).

The reduction in GAD67+ neurons without change to PV+ neurons could be due to a subset of GABA interneurons other than PV being affected. The findings of François et al. in 2009, who showed no differences in CR or calbindin neuron counts in the PFC of adult nVH lesion animals, suggest it may be SST neurons that are altered – although neuron numbers for any subtype in adolescence were not investigated. Reductions to SST neuron numbers have been found in human schizophrenia subjects post-mortem, as well as lower mRNA levels of the transcription factor Lhx6, which regulates SST and PV neuron development (Volk et al., 2014). These findings suggest that SST may be vulnerable in schizophrenia.

On the other hand, Hashimoto et al. (2003) found that GAD67 mRNA was absent in 50% of PV+ neurons in the PFC of patients with schizophrenia post-mortem. This suggests that PV+ neuron numbers could be unaltered, but GAD67 expression, and thus GABA function, is lost. Indeed, in the DISC-1 mouse model of schizophrenia, a reduction in both PV+ neurons and GAD67+/PV+ neurons was found in the adult mPFC (Lee et al., 2013). In the current study, GAD67+ neuron numbers are equal to those in sham animals by adulthood, despite previous research finding a reduction in GAD67 mRNA in adults, both rats and humans. It is possible that GAD67 expression is reduced while still being detectable for cell counting.

The relative staining quality of the PV antibody compared to the GAD67 antibody means that counting was clearer for PV+ neurons in the PFC, but the number of neurons counted as

expressing PV is generally in accordance with the typical distribution of PV in the cortex (~50% of GAD67-expressing neurons should express PV; DeFelipe et al., 2013). However, PV is characteristic for its late expression in development, as PV staining does not appear in prefrontal interneurons until around two weeks in rodents, and the precise timing has not been investigated in rats (Mukhopadhyay et al., 2009). In this study, it was found that PV+ neurons at PD20 across the PFC were not yet at the adult levels counted at PD60 ($p<0.0021$). Unpublished observations from this lab found that these levels are typically reached around PD25 in rats. Differences in maturation rate across animals may account for the high variability seen in PV counts for each group. There may not be a detectable difference between PV+ neurons in sham and lesion animals at this age because the expression profiles of the neurons are still being developed. However, GAD67+ neuron counts in the PFC are not significantly different at PD20 and PD60, suggesting that GAD67 expression reaches adult levels before PD20.

Reticular Thalamus

There was dramatic cell loss in the Rt of over 50% of the neurons at both PD20and PD60 in nVH lesion animals, with the curve of the C lost at both age groups. This area of the Rt is known to receive inputs from barrel, auditory, and visual cortices but other specific connections are unknown, particularly between the Rt and the VH (Pinaut, 2004). A tracing study in 2008 found that the rostral tail of the Rt receives connections from subiculum, but it was not specified whether this was the dorsal or ventral subiculum (Çavdar et al., 2008). The rostral section of the Rt also connects with the nucleus reuniens of the thalamus, one of the main relay centres between the hippocampal formation and higher brain regions (Çavdar et al., 2008). Disruption of these connections early in development may have led to the degradation of the Rt from loss of input.

Rt unbalance is associated is a common model for epilepsy and seizures, but no spontaneous seizures are seen in nVH lesion animals (Valdéz-Cruz et al., 2012). EEG measurements of freely moving adult lesion animals found lower alpha, beta, and theta band power but otherwise no unusual readings (Valdéz-Cruz et al., 2012). Sleep also appears to be unaffected in nVH lesion animals, though the Rt is responsible for the production of sleep spindles (Ferarrelli et al., 2010). Ahnaou et al (2007) found that nVH lesion animals have slower delta, theta and alpha wave power during sleep without overall disruption, but did not measure sleep spindle production.

It is difficult to conceive how this dramatic cell loss came about given what is known about the Rt. A loss of excitatory collaterals from VH and PFC would lead to increased inhibition in the Rt and excitatory imbalance, but not excitatory toxicity. It cannot be ignored that the ibotenic acid lesions may have been too dorsal and captured the caudal end of the Rt. However, the internal thalamic nuclei which the Rt surrounds do not appear damaged to the same extent. Additionally, in a rat model of stroke, central cerebral occlusion led to 45% cell loss in the Rt through secondary neuronal degradation due to astrocyte/glial activity (Dihné et al., 2002). It is possible that the nearby brain trauma of a lesion caused an increase in edema fluid around the Rt, which can produce neural damage and glial activation (Dihné et al., 2002). In fact, 36% of PV+ neurons were lost in the Rt following experimental traumatic brain injury, particularly as the nucleus progressed caudally (Huusko and Pitkänen, 2014). These are parallels which support the idea that cell loss can occur in this delicate nucleus after brain injury or trauma.

Future Research

Within the PFC, analysis of numbers of PV+ chandelier versus basket cells would provide valuable input into selective changes to GABA neuron cell types. Additionally, to better

understand the GAD67+ neuron reduction seen at PD20, GAD67+/PV+ dual staining and SST+ neurons in the prelimbic area and total PFC at PD20 and PD60 should be counted. A larger sample size would be valuable to more accurately capture and compare neuron counts in the PFC.

For the Rt, it is important to investigate whether the VH connects to the Rt directly, particularly around PD7 when the nVH lesion is performed. If there are no direct connections, the dramatic cell loss observed here must be interpreted through secondary mechanisms of action. To this end, it would be valuable to record the electrophysiological properties of the inner thalamic nuclei – particularly reuniens, which connects with both VH and the Rt (Çavdar et al., 2008), and the lateral nuclei nearest to the Rt – in lesion animals. This would elucidate changes to the neurons in areas to which the Rt directly projects and which would be most affected after loss of this nucleus. Finally, sleep spindles should be measured in nVH lesion animals to measure whether basic functionality of the Rt is still present.

Conclusions

This study found no significant change in PV+ neuron counts in the PFC before or after onset of schizophrenia-like behaviour, but GAD67+ neurons were reduced before behavioural onset in the prelimbic area only, suggesting that another GABA subtype may be affected at this age, or that a PV staining profile is maintained while GABA functionality is affected in other ways. It was also found that GAD67+, but not PV+, neurons are at adult levels by PD20.

A dramatic loss of >50% of the cells in the Rt of lesion animals was seen both before and after behavioural changes. This is an important nucleus for modulating and regulating information transfer between the PFC, hippocampus and thalamus, along with other higher-order brain regions. Recent schizophrenia literature (2012 to present) has had increasing focus on the

Rt, as its modulating role and diffuse connections implicate it in concepts of consciousness, auditory gating, and other behaviours known and affected in schizophrenia. Going forward, the PFC-thalamus-hippocampus circuit should be a promising area of future studies in schizophrenia research.

Appendix

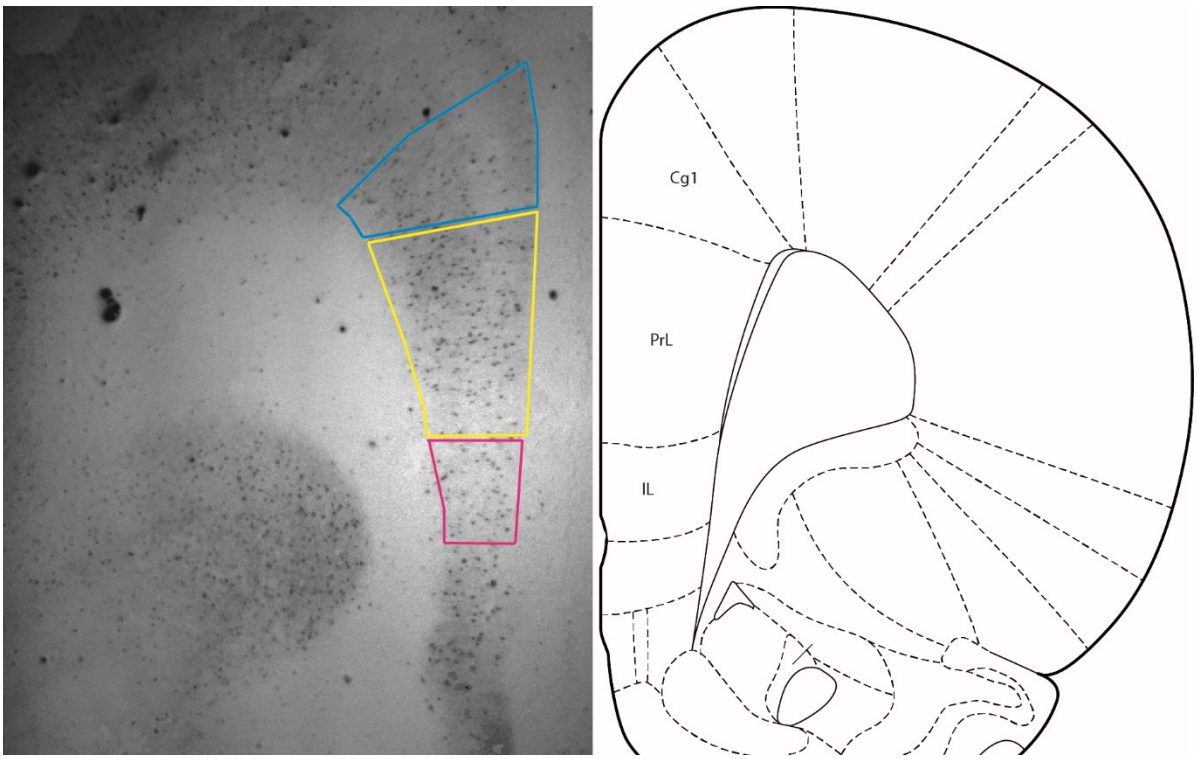

Figure 1a. Example of a typical tracing of the PFC subregions in Stereoinvestigator at 1x, using the Rat Brain Atlas as a guide (plate 11; Paxinos and Watson, 2005). IL=infralimbic, pink; PrL=Prelimbic, yellow; Cg1=cingulate, blue.

	CG		PL		IL	
	sham	lesion	sham	lesion	sham	lesion
PD20	8370.69	8715.29	8484.54	8454.96	1616.98	3487.94
	8721.22	5870.80	11491.45	5838.71	3910.61	2185.31
	9845.75	7955.85	12504.76	7789.68	6390.87	3530.45
	5631.89	8052.30	7494.93	12797.99	3522.30	4681.80
	7817.16	8333.71	7919.43	8074.47	2235.70	2789.23
	8241.40	4929.10	9949.92	4378.66	3260.94	2212.72
	8744.34	7034.39	11526.51	7115.25	5749.02	3324.75
	5102.44	10670.02	7550.45	10799.72	3168.78	3766.97
AVG	7809.36	7695.18	9615.25	8156.18	3731.90	3247.40
PD60	4182.08	6093.06	12025.20	9542.88	6833.88	4020.24
	7949.42	10286.20	11601.49	16976.39	6011.53	8388.25
	5069.12	10354.83	7867.50	14413.70	6083.14	6360.68
	6453.00	4612.22	15802.08	12171.12	6256.89	4536.60
	9073.96	8660.09	15368.63	17034.54	5642.33	7104.06
	4951.83	10722.63	9918.08	16157.67	3287.78	7719.11
	9865.39	5740.86	16258.71	12874.00	8658.66	4301.16
	7128.42	5681.89	10778.93	14790.42	5175.49	5599.40
AVG	6834.15	7768.97	12452.58	14245.09	5993.71	6003.69

Table 1. Raw data of PV+ counts in the PFC from 4 sham and 4 lesion animals per age point

	CG		PL		IL	
	sham	lesion	sham	lesion	sham	lesion
PD20	10819.85	7685.67	22914.37	11562.19	8535.17	6579.20
	10798.00	9562.39	20286.18	17795.96	9550.16	9177.14
	9004.43	10185.48	15204.46	16551.46	8899.64	11914.12
	9504.09	5603.25	16942.56	11333.26	9294.53	5693.08
	11396.96	6692.22	22350.88	14123.00	7488.14	8433.78
	11055.81	9764.95	19871.81	17505.42	9513.40	11386.79
	8036.34	7264.08	14367.35	16556.16	9610.47	12414.96
	8086.56	7685.67	15959.91	11562.19	11255.99	6579.20
AVG	9837.76	8055.46	18487.19	14623.71	9268.44	9022.28
PD60	15738.52	6762.85	27970.63	21108.05	10769.17	11185.18
	9690.99	16552.88	16076.25	30579.54	7147.10	16914.86
	5850.36	9511.82	13252.11	20409.56	7648.30	10782.77
	8767.56	7863.66	18542.81	13313.57	9610.14	6295.63
	13700.27	5126.89	26885.59	11007.45	11888.59	6847.25
	10450.55	16023.04	14296.83	30945.41	5915.10	15832.29
	9388.37	9610.58	19875.60	19200.86	9667.32	8041.52
	7761.57	7395.51	15795.62	15315.43	7051.44	4788.34
AVG	10168.52	9855.90	19086.93	20234.98	8712.15	10085.98

Table 2. Raw data of GAD67+ counts in the PFC from 4 sham and 4 lesion animals per age point

	PD20		PD60	
Rt counts	sham	lesion	sham	lesion
	85876.58	75627.63	84095.88	34665.11
	98616.66	40964.46	108043.84	18121.88
	84315.95	56258.34	128125.13	5566.46
	108341.20	46969.91	139925.95	71479.51
	86607.79	45934.11	84379.63	43037.02
	112015.02	47175.27	109333.95	31341.03
	95027.53	55366.73	135789.73	12941.76
	85908.40	33772.48	137252.75	49714.98
AVG	94588.64	50258.62	115868.36	33358.47

Table 3. Raw data of PV+ counts in the Rt from 4 sham and 4 lesion animals per age point

	PD20		PD60	
Rt counts	sham	lesion	sham	lesion
	48472.33	36430.80	78217.66	28801.15
	60618.70	33077.66	76310.39	11102.16
	66992.29	43538.61	99854.54	15242.37
	72951.67	29185.07	38601.30	45791.86
	47152.98	26449.57	71317.39	23243.97
	71012.34	20657.24	76130.61	14153.93
	73189.57	34134.27	82436.03	14170.30
	58764.21	19076.71	33370.64	37869.74
AVG	62394.26	30318.74	69529.82	23796.94

Table 4. Raw data of GAD67+ counts in the Rt from 4 sham and 4 lesion animals per age point

	Sham	Lesion
PD20	53567.40	80591.93
	80179.34	75591.6
	110410.20	50147.94
	130712.85	32619.78
PD60	70564.98	12904.93
	75106.6	16042.47
	76454.98	22366.07
	72390.12	20045.73
AVG	73629.17	17839.8

Table 5. Raw data of NeuN+ counts in the Rt from 4 sham and 4 lesion animals

References

Ahnaou A, Nayak S, Heylen A, Ashton D, Drinkenburg WH (2007) Sleep and EEG profile in neonatal hippocampal lesion model of schizophrenia. Physiol Behav 92(3):461-7.

Arai R, Jacobowitz DM, Deura S (1994) Distribution of calretinin, calbindin-D28k, and parvalbumin in the rat thalamus. Brain Res Bul 33(5):595-614.

Bartos M, Vida I, Jonas P (2007) Synaptic mechanisms of synchronized gamma oscillations in inhibitory interneuron networks. Nat Rev Neurosci 8(1):45-56.

Behrendt RP (2006) Dysregulation of thalamic sensory "transmission" in schizophrenia: neurochemical vulnerability to hallucinations. J Psychopharmacol 20(3):356-72.

Bitanihirwe BK, Lim MP, Kelley JF, Kaneko T, Woo TU (2009) Glutamatergic deficits and parvalbumin-containing inhibitory neurons in the prefrontal cortex in schizophrenia. BMC Psychiatry. 9:71.

Bitanihirwe BK, Woo TU (2014) Transcriptional dysregulation of γ-aminobutyric acid transporter in parvalbumin-containing inhibitory neurons in the prefrontal cortex in schizophrenia. Psychiatry Res. 220(3):1155-9.

Blum BP, Mann JJ (2002) The GABAergic system in schizophrenia. Int J Neuropsychopharmacol 5(2):159-79.

Çavdar S, Onat FY, Cakmak YO, Yananli HR, Gülçebi M, Aker R (2008) The pathways connecting the hippocampal formation, the thalamic reuniens nucleus and the thalamic reticular nucleus in the rat. J Anat. 212(3):249-56.

Curley AA, Lewis DA (2012) Cortical basket cell dysfunction in schizophrenia. J Physiol 590(Pt 4):715-24.

Curley AA, Eggan SM, Lazarus MS, Huang ZJ, Volk DW, Lewis DA (2013) Role of glutamic acid decarboxylase 67 in regulating cortical parvalbumin and GABA membrane transporter 1 expression: implications for schizophrenia. Neurobiol Dis 50:179-86.

Dalley JW, Cardinal RN, Robbins TW (2004) Prefrontal executive and cognitive functions in rodents: neural and neurochemical substrates. Neurosci Biobehav Rev 28(7):771-84.

DeFelipe J, López-Cruz PL, Benavides-Piccione R, Bielza C, Larrañaga P, Anderson S, Burkhalter A, Cauli B, Fairén A, Feldmeyer D, Fishell G, Fitzpatrick D, Freund TF, González-Burgos G, Hestrin S, Hill S, Hof PR, Huang J, Jones EG, Kawaguchi Y, Kisvárday Z, Kubota Y, Lewis DA, Marín O, Markram H, McBain CJ, Meyer HS, Monyer H, Nelson SB, Rockland K, Rossier J, Rubenstein JL, Rudy B, Scanziani M, Shepherd GM, Sherwood CC, Staiger JF, Tamás

G, Thomson A, Wang Y, Yuste R, Ascoli GA (2013) New insights into the classification and nomenclature of cortical GABAergic interneurons. Nat Rev Neurosci 14(3):202-16.

Dihné M, Grommes C, Lutzenburg M, Witte OW, Block F (2002) Different mechanisms of secondary neuronal damage in thalamic nuclei after focal cerebral ischemia in rats. Stroke 33(12):3006-11.

Egerton A, Reid L, McKerchar CE, Morris BJ, Pratt JA (2005) Impairment in perceptual attentional set-shifting following PCP administration: a rodent model of set-shifting deficits in schizophrenia. Psychopharmacology (Berl) 179(1):77-84.

Endo K, Hori T, Abe S, Asada T (2007) Alterations in GABA(A) receptor expression in neonatal ventral hippocampal lesioned rats: comparison of prepubertal and postpubertal periods. Synapse 61(6):357-66.

Fallon JH, Opole IO, Potkin SG (2003) The neuroanatomy of schizophrenia: circuitry and neurotransmitter systems. Clin Neurosci Res 3:77–107.

Ferrarelli F, Peterson MJ, Sarasso S, Riedner BA, Murphy MJ, Benca RM, Bria P, Kalin NH, Tononi G (2010) Thalamic dysfunction in schizophrenia suggested by whole-night deficits in slow and fast spindles. Am J Psychiatry 167(11):1339-48.

Ferrarelli F, Tononi G (2011) The thalamic reticular nucleus and schizophrenia. Schizophr Bull 37(2):306-15.

Flores G, Barbeau D, Quirion R, Srivastava LK (1996) Decreased binding of dopamine D3 receptors in limbic subregions after neonatal bilateral lesion of rat hippocampus. J Neurosci 16(6):2020-6.

Flores G, Silva-Gómez AB, Ibáñez O, Quirion R, Srivastava LK (2005) Comparative behavioral changes in postpubertal rats after neonatal excitotoxic lesions of the ventral hippocampus and the prefrontal cortex. Synapse 56(3):147-53.

François J, Ferrandon A, Koning E, Angst MJ, Sandner G, Nehlig A (2009) Selective reorganization of GABAergic transmission in neonatal ventral hippocampal-lesioned rats. Int J Neuropsychopharmacol 12(8):1097-110.

Gandal MJ, Nesbitt AM, McCurdy RM, Alter MD (2012) Measuring the maturity of the fast-spiking interneuron transcriptional program in autism, schizophrenia, and bipolar disorder. PLoS One 7(8):e41215

Godsil BP, Kiss JP, Spedding M, Jay TM (2013) The hippocampal-prefrontal pathway: the weak link in psychiatric disorders? Eur Neuropsychopharmacol 23(10):1165-81.

Gogtay N, Giedd JN, Lusk L, Hayashi KM, Greenstein D, Vaituzis AC, Nugent TF 3rd, Herman DH, Clasen LS, Toga AW, Rapoport JL, Thompson PM (2004) Dynamic mapping of human cortical development during childhood through early adulthood. Proc Natl Acad Sci U S A 101(21):8174-9.

Gonzales-Burgos G, Fish KN, Lewis DA (2011) GABA neuron alterations, cortical circuit dysfunction and cognitive deficits in schizophrenia. Neural Plast 2011:723184.

Grillon ML, Oppenheim C, Varoquaux G, Charbonneau F, Devauchelle AD, Krebs MO, Baylé F, Thirion B, Huron C (2013) Hyperfrontality and hypoconnectivity during refreshing in schizophrenia. Psychiatry Res 211(3):226-33.

Harrison PJ (2004) The hippocampus in schizophrenia: a review of the neuropathological evidence and its pathophysiological implications. Psychopharmacology (Berl) 174(1):151-62.

Hashimoto T, Volk DW, Eggan SM, Mirnics K, Pierri JN, Sun Z, Sampson AR, Lewis DA (2003) Gene expression deficits in a subclass of GABA neurons in the prefrontal cortex of subjects with schizophrenia. J Neurosci 23(15):6315-26.

Hashimoto T, Bazmi HH, Mirnics K, Wu Q, Sampson AR, Lewis DA (2008) Conserved regional patterns of GABA-related transcript expression in the neocortex of subjects with schizophrenia. Am J Psychiatry 165:479–489.

Heidbreder CA, Groenewegen HJ (2003) The medial prefrontal cortex in the rat: evidence for a dorso-ventral distinction based upon functional and anatomical characteristics. Neurosci Biobehav Rev 27(6):555-79.

Hinkley LB, Vinogradov S, Guggisberg AG, Fisher M, Findlay AM, Nagarajan SS (2011) Clinical symptoms and alpha band resting-state functional connectivity imaging in patients with schizophrenia: implications for novel approaches to treatment. Biol Psychiatry 70(12):1134-42.

Huusko N, Pitkänen A (2014) Parvalbumin immunoreactivity and expression of GABAA receptor subunits in the thalamus after experimental TBI. Neuroscience. 267:30-45.

Jiang Z, Cowell RM, Nakazawa K (2013) Convergence of genetic and environmental factors on parvalbumin-positive interneurons in schizophrenia. Front Behav Neurosci 7:116.

Jovanovic JN, Thomson AM (2011) Development of cortical GABAergic innervation. Front Cell Neurosci 5:14.

Kamath A, Al-Khairi I, Bhardwaj S, Srivastava LK (2006) Enhanced alpha1 adrenergic sensitivity in sensorimotor gating deficits in neonatal ventral hippocampus-lesioned rats. Int J Neuropsychopharmacol 11(8):1085-96.

Kendler KS (2014) A joint history of the nature of genetic variation and the nature of schizophrenia. Mol Psychiatry doi: 10.1038/mp.2014.94.

Mukhopadhyay A, McGuire T, Peng CY, Kessler JA (2009) Differential effects of BMP signaling on parvalbumin and somatostatin interneuron differentiation. Development 136(15):2633-42.

Lee FH, Zai CC, Cordes SP, Roder JC, Wong AH (2013) Abnormal interneuron development in disrupted-in-schizophrenia-1 L100P mutant mice. Mol Brain 6:20.

Lipska BK (2004) Using animal models to test a neurodevelopmental hypothesis of schizophrenia. J Psychiatry Neurosci 29(4): 282–286.

Lipska BK, Weinberger DR (2000) To model a psychiatric disorder in animals: schizophrenia as a reality test. Neuropsychopharmacology 23:223–239.

Majak K, Berdel B, Kowiański P, Dziewiatkowski J, Lipowska M, Moryś J (1998) Parvalbumin immunoreactivity changes in the thalamic reticular nucleus during the maturation of the rat's brain. Folia Neuropathol 36(1):7-14.

McDannald MA, Whitt JP, Calhoon GG, Piantadosi PT, Karlsson RM, O'Donnell P, Schoenbaum G (2011) Impaired reality testing in an animal model of schizophrenia. Biol Psychiatry 70(12):1122-6.

Min BK (2010) A thalamic reticular networking model of consciousness. Theor Biol Med Model 7:10-27.

Nakazawa K, Zsiros V, Jiang Z, Nakao K, Kolata S, Zhang S, Belforte JE (2012) GABAergic interneuron origin of schizophrenia pathophysiology. Neuropharmacology 62(3):1574-83.

Nikolaus S, Hautzel H, Müller HW (2014) Focus on GABAA receptor function. A comparative analysis of in vivo imaging studies in neuropsychiatric disorders. Nuklearmedizin 53(6):227-37.

Ohnuma T, Augood SJ, Arai H, McKenna PJ, Emson PC (1999) Measurement of GABAergic parameters in the prefrontal cortex in schizophrenia: focus on GABA content, GABA(A) receptor alpha-1 subunit messenger RNA and human GABA transporter-1 (HGAT-1) messenger RNA expression. Neuroscience 93(2):441-8.

Ohtani T, Levitt JJ, Nestor PG, Kawashima T, Asami T, Shenton ME, Niznikiewicz M, McCarley RW (2014) Prefrontal cortex volume deficit in schizophrenia: a new look using 3T MRI with manual parcellation. Schizophr Res 152(1):184-90.

Paxinos G, Watson C (2005). The Rat Brain in Stereotaxic Coordinates – 5th edition. Academic Press, San Diego, CA.

Perry TL, Kish SJ, Buchanan J, Hansen S (1979) Gamma-aminobutyric-acid deficiency in brain of schizophrenic patients. Lancet 1(8110):237-9.

Pinal CS, Tobin AJ (1998) Uniqueness and redundancy in GABA production. Perspect Dev Neurobiol 5(2-3):109-18.

Pinault D (2004) The thalamic reticular nucleus: structure, function and concept. Brain Res Brain Res Rev 46(1):1-31.

Povysheva NV, Zaitsev AV, Gonzalez-Burgos G, Lewis DA (2013) Electrophysiological heterogeneity of fast-spiking interneurons: chandelier versus basket cells. PLoS One 8(8):e70553.

Selemon LD, Kleinman JE, Herman MM, Goldman-Rakic PS (2002) Smaller frontal gray matter volume in postmortem schizophrenic brains. Am J Psychiatry 159(12):1983-91.

Sun Y, Farzan F, Barr MS, Kirihara K, Fitzgerald PB, Light GA, Daskalakis ZJ (2011) γ oscillations in schizophrenia: mechanisms and clinical significance. Brain Res 1413:98-114.

Torres-García ME1, Solis O, Patricio A, Rodríguez-Moreno A, Camacho-Abrego I, Limón ID, Flores G (2012) Dendritic morphology changes in neurons from the prefrontal cortex, hippocampus and nucleus accumbens in rats after lesion of the thalamic reticular nucleus. Neuroscience 223:429-38.

Troyano-Rodriguez E, Lladó-Pelfort L, Santana N, Teruel-Martí V, Celada P, Artigas F (2014) Phencyclidine inhibits the activity of thalamic reticular gamma-aminobutyric acidergic neurons in rat brain. Biol Psychiatry 76(12):937-45.

Tseng KY, Chambers RA, Lipska BK (2009) The neonatal ventral hippocampal lesion as a heuristic neurodevelopmental model of schizophrenia. Behav Brain Res 204(2):295-305

Tseng KY, Lewis BL, Hashimoto T, Sesack SR, Kloc M, Lewis DA, O'Donnell P (2008) A neonatal ventral hippocampal lesion causes functional deficits in adult prefrontal cortical interneurons. J Neurosci 28(48):12691-9.

Valdés-Cruz A, Negrete-Díaz JV, Magdaleno-Madrigal VM, Martínez-Vargas D, Fernández-Mas R, Almazán-Alvarado S, Torres-García ME, Flores G (2012) Electroencephalographic activity in neonatal ventral hippocampus lesion in adult rats. Synapse 66(8):738-46.

Vertes RP (2004) Differential projections of the infralimbic and prelimbic cortex in the rat. Synapse 51(1):32-58.

Volk D, Austin M, Pierri J, Sampson A, Lewis D (2001) GABA transporter-1 mRNA in the prefrontal cortex in schizophrenia: decreased expression in a subset of neurons. Am J Psychiatry 158(2):256-65.

Volk DW, Edelson JR, Lewis DA (2014) Cortical inhibitory neuron disturbances in schizophrenia: role of the ontogenetic transcription factor Lhx6. Schizophr Bull 40(5):1053-61.

Volk DW, Radchenkova PV, Walker EM, Sengupta EJ, Lewis DA (2012) Cortical opioid markers in schizophrenia and across postnatal development. Cereb Cortex 22(5):1215-23.

Woodward ND, Duffy-Alberto B, Karbasforoushan H (2013) Prefrontal cortex activity during response selection predicts processing speed impairment in schizophrenia. J Int Neuropsychol Soc 19(7): 782–791.

Zikopoulos B, Barbas H (2007) Circuits formultisensory integration and attentional modulation through the prefrontal cortex and the thalamic reticular nucleus in primates. Rev Neurosci 18(6):417-38.